Wildfire effects on stream metabolism: Aquatic succession is mediated by local riparian succession and stream geomorphology

Emily A. Davis

A thesis
Submitted in partial fulfillment of the
requirements for the degree of

Master of Science

University of Washington
2015

Committee:
Daniel Schindler
Christian Torgersen
Colden Baxter
Charles Simenstad

Program Authorized to Offer Degree:
School of Aquatic and Fishery Science

University of Washington

Wildfire effects on stream metabolism: Aquatic succession is mediated by local riparian succession and stream geomorphology

Emily A. Davis

Chair of the Supervisory Committee:
Dr. Daniel Schindler
School of Aquatic and Fishery Science

Abstract

As climate change shifts and intensifies fire regimes, it is important to understand stream ecosystem responses to fire. How stream metabolism responds remains largely unexplored. We investigated effects of fire severity and watershed geomorphology on stream ecosystem metabolism at multiple spatial scales in an Idaho wilderness watershed. We measured dissolved oxygen, temperature, and irradiance in 18 streams varying in fire history and watershed characteristics in order to model diel oxygen dynamics, from which we estimated rates of production (P) and respiration (R), then used P:R as an index of stream metabolic state. We found that post-fire riparian canopy recovery strongly influenced stream metabolic state. Severely burned streams with dense riparian regrowth were heterotrophic, whereas streams with less canopy recovery were autotrophic. Fire effects on stream metabolic state were highly mediated by watershed geomorphology, with the strongest long-term changes observed in low-order, narrow, steep streams. Effect sizes of fire and watershed geomorphology on stream metabolism changed from fine spatial scale (500-m riparian buffer) to coarse scale (watershed), and were strongest at fine scales. These results indicate that the physical habitat template mediates aquatic ecosystem response to disturbance, and that context and scale should be explicitly considered in assessments of ecosystem response to fire.

Table of Contents

List of Tables iv

List of Figures vi

Chapter 1: Wildfire effects on stream metabolism: Aquatic succession is mediated by local riparian succession and stream geomorphology ii

Abstract ii

Introduction 1

Methods 5

Study system and sites 6

Stream metabolism measurements 7

Environmental data 9

GIS methods 10

Metabolism modeling 12

Statistics 15

Results 16

Watershed geomorphology and burn history 16

Effects of geomorphology and burn history on stream chemistry and light conditions 17

Stream metabolism and stream chemistry 18

Spatial variation in effects of burn history and stream geomorphology on stream metabolism 20

Variation in stream chemistry, light and metabolism explained by burn history vs. geomorphology 21

Discussion 23

Figures 32

Tables 43

References 60

Acknowledgements 70

Appendix 1: Supplemental Figures 72

List of Tables

Table **Page**

Table 1. Results from response variables Principal Components Analysis (PCA) and explanatory variables PCA. The response variables PCA is based on stream chemical and light data collected from the 18 streams at the time of this study, while the explanatory variables PCA is based on fire history and geomorphic/physical data from the 18 streams. N:P = nitrogen: phosphorus ratio, DOC = dissolved organic carbon, TN = total nitrogen concentration, TP= total phosphorus concentration, TotalQ= stream discharge, AvgDepth= average depth, AvgWidth= average width, Low= percent burned with low severity, Area= watershed area, Slope= mean slope, PercentBurned= percent total watershed burned, Mod= percent burned with moderate severity, Severe= percent burned with high severity, VeryLow= percent burned with very low severity. *= significant axis based on 1000 random permutations. 43

Table 2a. Percent total watershed burned predicts total percent burned at other scales. 45

Table 2b. Percent total watershed burned predicts percent burned with high severity at some other scales 46

Table 3. Ranges of physical, geomorphic, and chemical characteristics of streams sampled in this study. TN = Total nitrogen; TP= Total phosphorus; N:P= Nitrogen to phosphorus ratio; DOC= Dissolved organic carbon; *Chl-a* = Chlorophyll-a. 47

Table 4. Principal Component Regressions. *= significant ($p \leq 0.05$), **= marginally significant ($0.25 \geq p > 0.05$). Response PC1 captures variation among streams in total nitrogen concentration and light, while Response PC2 captures variation in phosphorus concentration. PC1 and PC2 refer to the scale-specific principal components of the explanatory variables PCA; for each scale, PC1 captures variation in that scale's geomorphic characteristics, while PC2 captures the variation in burn history. GPP= gross primary production, Rt= total respiration, PR= ratio of gross primary production to total respiration. 48

Table 5. Metabolism parameters for each of 18 study streams. Respiration models: 1= No biological activity ([O2] governed only by physical parameters) ; 2= Temperature-sensitive CR using only one carbon substrate (Rb), using Equation 3; 3= Temperature- sensitive CR using only one carbon substrate and equation 6; 4= Constant CR, where CR is assumed not to respond to temperature; 5= Temperature-sensitive CR using two carbon sources (Rb and Rp) using photosynthesis from the previous timestep (Equation 4); 6= Temperature-sensitive CR using two carbon sources (Rb and Rp), calculated with a weighted average of the previous 30 minutes of estimated photosynthesis (Equation 5) 49

Table 6a. Range of models predicting the effect of burn history, watershed geomorphology, and their interaction on rates of gross primary productivity in streams in this study. Models were compared using AICc. βo = the estimated intercept, βn= the model- specific estimated slope of parameter *n*, N = sample size, k = number of parameters, SE= standard error. Δ AIC_c is the difference between each model-specific AIC_c value and the lowest AIC_c value within the set of

models in a given scale; and AIC_c w_i is the model weight for each model considered. Highlighted models are the top models (Δ AIC_c = 0) for a given scale..... 51

Table 6b. Range of models predicting the effect of burn history (PC2, PC3), watershed geomorphology (PC1), and their interaction on rates of total respiration in streams in this study. Models were compared using AIC_c. β_o = the estimated intercept, β_n= the model-specific estimated slope of parameter *n*, N = sample size, k = number of parameters, SE= standard error. Δ AIC_c is the difference between each model-specific AIC_c value and the lowest AIC_c value within the set of models in a given scale; and AIC_c w_i is the model weight for each model considered. Highlighted models are the top models (Δ AIC_c = 0) for a given scale……....53

Table 6c. Range of models predicting the effect of burn history (PC2, PC3), watershed geomorphology (PC1), and their interaction on rates of whole-stream metabolism (P:R) in streams in this study. Models were compared using AIC_c. β_o = the estimated intercept, β_n= the model-specific estimated slope of parameter *n*, N = sample size, k = number of parameters, SE= standard error. Δ AIC_c is the difference between each model-specific AIC_c value and the lowest AIC_c value within the set of models in a given scale; and AIC_c w_i is the model weight for each model considered. Highlighted models are the top models (Δ AIC_c = 0) for a given scale…….55

Table 7a. Total inertia (variance) in partial redundancy analysis. Total inertia= total variance in response matrix. Constrained inertia= inertia in response matrix explained by explanatory matrix; unconstrained inertia= unexplained inertia in response variables. 57

Table 7b. Components results from partial redundancy analysis. Components correspond to a single exclusive (non-overlapping) partition of total response variance. V1=pure effects from burn history matrix; v2= pure effects from geomorphology matrix; v12= joint burn history & geomorphology effects; confounded variance that cannot exclusively be associated with either v1 or v2. Proportion of total= partition size in terms of proportion of total response variance; Proportion of constrained= partition size in terms of proportion of total response variance explained by respective components. *= significant ($p \leq 0.05$), **= marginally significant ($0.25 \geq p > 0.05$)……58

Table 7c. Marginal effects results from partial redundancy analysis. Marginal effects are total variance in response matrix that can be attributable to a single explanatory matrix without partialling out the potential confounding effect of other explanatory matrices. V1= burn history matrix; v2= geomorphology matrix. Proportion of total = relative effect size given in terms of total response variance; Proportion of constrained = relative effect size in terms of total explained variance. P-values are based on a Monte Carlo test of significance with 1000 random permutations. *= significant ($p \leq 0.05$), **= marginally significant ($0.25 \geq p > 0.05$)……..59

List of Figures

Figure **Page**

Figure 1. Big Creek watershed, overlain by 18 subwatersheds of interest; study sites are marked by red points. Inset shows Big Creek's location in central Idaho, USA. 32

Figure 2. Principal component analysis for environmental data (stream geomorphology and burn history), watershed-scale 33

Figure 3. Percent variance explained by stream geomorphology versus burn history at each of ten scales of analysis. 34

Figure 4. Percent of the entire watershed burned almost perfectly predicts total percent riparian burned over the entire area of a given stream network's riparian buffer. Percent watershed burned also predicts the percent of the network's riparian buffer burned. 35

Figure 5. Principal component analysis of response variables (stream chemistry and light) from streams included in this study. 'PC'= principal component; value in parentheses indicates the percentage of variance explained by each axis. 'TN.TP'=ratio of total nitrogen to total phosphorus; 'DOC'=dissolved organic carbon; 'TN'=total nitrogen; 'TP'=total phosphorus. Open circles, which represent stream sites, are scaled by the mean width of the stream. 36

Figure 6a-b. Principal component regressions of response principal component 1 (light and nitrogen concentration) against explanatory principal component 1 (stream geomorphology) for the coarsest (watershed scale) and finest (500-m riparian buffer) spatial resolution in this study. 'PC'= principal component. Open circles, which represent streams, are scaled by the mean width of the stream. 37

Figure 7. Principal component regression of response principal component 1 (light and nitrogen concentration) against the logged values of estimated gross primary productivity (GPP) for each study stream. 'PC'= principal component. Open circles, which represent streams, are scaled by the mean width of the stream. 38

Figure 8. Principal component regression of response principal component 1 (light and nitrogen concentration) against the logged values of estimated whole-stream metabolism (P:R) for each stream for which a respiration value could be estimated. 'PC'= principal component. Open circles, which represent streams, are scaled by the mean width of the stream. 39

Figure 9. Principal component regression of response principal component 2 (phosphorus concentration) against the logged values of total respiration (Rt) for each stream for which a respiration value could be estimated. 'PC'= principal component. Open circles, which represent streams, are scaled by the mean width of the stream. 40

Figure 10 a-c. Effect size of environmental principal component 1 (stream geomorphology) and principal component 2 (burn history) plotted against scale of analysis (1=500-m riparian buffer,

2= 1000-m riparian buffer, and so on up to 9=network-scale riparian buffer, 10=watershed scale), from regressions against each of three response variables: a) gross primary productivity (GPP); b) total respiration (Rt); and c) whole-stream metabolism (P:R). 41

Figure 11. Results of partial redundancy analysis (pRDA): Marginal effects (variance attributable to single explanatory data sets without partialling out joint or confounding variation) of stream geomorphology vs. burn history on the response matrix, at each of ten spatial scales 42

Supplemental Figure 1 a-j. Principal component analyses for environmental data (stream geomorphology and burn history) for each of 10 spatial resolutions: a) 500-m riparian buffer (PC1 43.57%, PC2 22.91%); b) 1000-m riparian buffer (PC1 43.74%, PC2 20.32%); c) 1500-m riparian buffer (PC1 42.79%, PC2 20.33%); d) 2000-m riparian buffer (PC1 43.86%, PC2 22.5%); e) 2500-m riparian buffer (PC1 43.91%, PC2 22.91%); f) 3000-m riparian buffer (PC1 47.44%, PC2 23.41%); g) 3500-m riparian buffer (PC1 44.35%, PC2 25.46%); h) 4000-m riparian buffer (PC1 43.85%, PC2 26.4%); i) network-scale riparian buffer (PC1 58.25%, PC2 16.42%); j) watershed scale (PC1 60.85%, PC2 15.9%). 'PC'= principal component. All vectors shown are significant. 'TotalQ'=stream discharge; 'AvgWidth'= mean stream width; 'AvgDepth'=mean stream depth; 'Slope'=mean slope over study area; 'PercentLow'=percent area burned with low severity; 'PercentMod'=percent area burned with moderate severity; 'PercentSevere'=percent area burned with high severity; 'PercentUB'=percent area burned with very low severity. Open circles, which represent stream sites, are scaled by the mean width of the stream…….72

Supplemental Figure 2 a-h. Percent watershed burned plotted against total percent of riparian buffer burned, and percent of buffer burned at high severity, over 8 spatial scales of riparian buffer: a) 500-m; b) 1000-m; c) 1500-m; d) 2000-m; e) 2500-m; f) 3000-m; g) 3500-m h) 4000-m……73

Supplemental Figure 3a-j. Principal component regressions of response principal component 1 (light and nitrogen concentration) against explanatory principal component 1 (stream geomorphology) for each of ten spatial scales of analysis: a) watershed; b) network-scale riparian buffer; c) 4000-m riparian buffer; d) 3500-m riparian buffer; e) 3000-m riparian buffer; f) 2500-m riparian buffer; g) 2000-m riparian buffer; h) 1500-m riparian buffer; i) 1000-m riparian buffer; j) 500-m riparian buffer. 'PC'= principal component. Open circles, which represent streams, are scaled by the mean width of the stream…….74

Chapter 1: Wildfire effects on stream metabolism: Aquatic succession is mediated by local riparian succession and stream geomorphology

Introduction

Wildfire is an important agent of natural disturbance in lotic systems, due to the many ways in which it can change the degree and nature of aquatic-terrestrial connectivity (Gresswell 1999). In his classic 1999 synthesis, Gresswell presented a conceptual model adapted from Minshall et al. (1989) of the post-fire response trajectories of stream ecosystems. The general hypothesis developed by this model is that stream productivity recovers in the first few years following a burn and increases to levels higher than those observed pre-fire within the first decade following disturbance, then returns to background levels over the following decades. The key variables driving this response are presumed to be changing conditions of light and nutrients, though until recently little mechanistic work has been done to evaluate these assumptions. Some of the hypotheses about recovery trajectories have been supported, specifically in work on invertebrate productivity in the mid-term after fire (Malison and Baxter 2010b) and observations of long-term recovery in Yellowstone National Park (Romme et al. 2011). Though much is now known about effects of fire on sediment dynamics, nutrient input, and fish and macroinvertebrate communities, comparatively little is known about fire impacts on the functional ecosystem processes—such as primary production and community respiration—that support stream biota. Furthermore, although much is known about the immediate and short-term effects of fire (i.e., on time scales of days to months), much less is known about recovery trajectories in the mid- and long-term after fire (time scales of years to decades) (Gresswell 1999). Study of mid- and long-term recovery trajectories is important for understanding processes of succession both within the

stream, and in the upland and riparian areas that influence the stream, after wildfire disturbance (Malison and Baxter 2010b).

Stream metabolic state, a holistic metric that integrates the consumption and production of energy within the stream, has long been used by ecologists to interpret stream responses to disturbances ranging from agriculture and logging (Mulholland et al. 2001, Bernot et al. 2010, Griffiths et al. 2013), to floods (Uehlinger et al. 2003, Robinson et al. 2004, Robinson and Uehlinger 2008), and the activity of ecosystem engineers such as spawning salmon (Holtgrieve and Schindler 2011). A large body of work suggests that light is one of the main drivers of stream ecosystem metabolism often affected by disturbances such as wildfire. Light in stream ecosystems is predominantly controlled (at least in forested biomes) by the degree of riparian cover (Kiffney et al. 2003, 2004, Cole and Newton 2013, Newton and Cole 2013). Further, incident photosynthetically active radiation (PAR) drives GPP (Young and Huryn 1996, 1999, Rutherford et al. 2004, Fellows et al. 2006); thus, riparian vegetation is an important mediator of GPP (Mulholland et al. 2001, Acuna et al. 2004, McTammany et al. 2007). If riparian cover is reduced by disturbance, stream metabolism may increase, usually driven by an increase in GPP (Bunn et al. 1998b, a, Bunn et al. 1999, Mosisch et al. 2001). If ER is dependent on photosynthetic carbon, a disturbance-induced reduction in riparian cover may also lead to an increase in ER (Yates et al. 2013). However, this response is time and context-dependent: Regrowth and recovery of the riparian zone over decades has been shown to drive GPP down to levels similar to pre-disturbance (McTammany et al. 2007), but this may depend on stream-specific attributes such as size or slope.

Wildfire disturbance is likely to have a similar effect on stream metabolism. Some researchers have speculated that increases in post-fire secondary productivity were due to

changes in primary productivity and stream metabolism (Malison and Baxter 2010a, b). While algal biomass, diatom production and invertebrate production have been assessed in numerous studies of wildfire disturbance (reviewed in Gresswell 1999), only two studies focus on the effects of wildfire on whole-stream metabolism (Tuckett 2007, Betts and Jones 2009), while an additional study examines only post-fire rates of benthic and sediment respiration (Robinson et al. 2005). Taken together, these few studies indicate that wildfire, like other disturbances, can alter whole-stream metabolism, but do not provide a clear answer as to the magnitude, timing, or direction of the response, or the driving mechanism behind it.

Because of the important role riparian vegetation plays in mediating stream primary productivity via light and, to a lesser degree, nutrient cycling (Pettit and Naiman 2007), the overall effect of wildfire on stream ecosystems is probably predicated to a large degree on whether the riparian canopy burns, the intensity of the burn, and the manner and speed of its recovery (Dwire and Kauffman 2003, Pettit and Naiman 2007, Verkaik et al. 2013). Where riparian vegetation burns, there is less canopy cover, higher temperatures, more aquatic algal biomass, more algivores, and a higher degree of autochthony (Cooper et al. 2014). Pronounced changes in nutrient loads after fire tend to have a short-term impact; after vegetation begins to regrow (if it begins to regrow at all), increased erosion and runoff that add sediment and nutrients to streams level off and normalize. However, postfire riparian recovery can impact stream nutrient cycling over the longer term (Pettit and Naiman 2007) and is, therefore, worth taking into account alongside light as a potential co-driver of long term stream recovery. Furthermore, not all fires are the same. For example, the intensity of fire effects on the stream has more to do with the severity of the burn in the riparian zone than whether or not it burned at all; severely burned riparian areas are much likelier to display a detectable effect of fire (Arkle

and Pilliod 2010). Because of this, fire severity may determine the magnitude of effect on stream productivity and subsequent energy transfer through food webs, making studies of response across a severity gradient important (Malison and Baxter 2010a).

Gresswell's conceptual model imagines post-fire response trajectories at a single point in an idealized stream over time, and indeed, most studies of wildfire effects on stream ecosystems have occurred at the spatial scale of stream reaches. However, studies at this scale may miss relevant ecological responses, as processes of succession in lotic systems occur not only temporally but also longitudinally (Odum 1956), due to shifting relative importance of light and nutrients along the stream continuum (Vannote et al. 1980, Finlay 2011, Finlay et al. 2011). Investigating disturbance effects at a single scale may provide an incomplete picture, as ecological responses can change in magnitude or direction with different observational scales (Rieman et al. 2006). The cumulative effect of fire over a landscape may impact a stream network in non-linear, non-additive ways, particularly if fire over one area has downstream impacts to another area, but little work has been attempted on this topic.

How will stream recovery from wildfire proceed across a continuum of space? We know from an increased emphasis on study of streams as spatially heterogeneous networks that streams vary widely in their physical habitat characteristics across the riverscape (Frissell et al. 1986, Fausch et al. 2002, Benda et al. 2004). Because streams vary physically, they will not all respond to disturbance similarly. For example, variation in reach geomorphology along a stream is one factor that can mediate the impact of riparian shading (or the lack thereof) on local stream metabolism (Bott et al. 2006).

Streams are intimately related to their watersheds (Hynes 1974), but there have been no efforts to understand the spatial scales at which fires affect stream metabolic processes, and

whether these scaling relationships are affected by watershed geomorphic conditions. The study of aquatic-terrestrial connectivity has expanded from investigating terrestrial conditions at a very local scale to consideration of the entire watershed (Peterson et al. 2011). Land in closer physical proximity to a stream, or land that is more hydrologically connected to a stream has a disproportionate effect on the stream ecosystem compared to more distant upland (Peterson et al. 2011). For this reason, using a "lumped" metric of land cover at a coarse, whole-watershed scale can be misleading or uninformative (Peterson et al. 2011). In a study of the spatial scale of land use that most strongly affects a river's various ecological health indicators (Sheldon et al. 2012), riparian cover at a scale close to a stream site (in a buffer zone, for example) were overwhelmingly the most important spatial scale and predictor (respectively) of stream ecosystem health and function. Importantly, this study also found that ecosystem indicators are commonly explained by a combination of scales (Sheldon et al. 2012).

In this paper, we inform three important knowledge gaps in the study of wildfire and lotic systems: (1) disturbance effects on ecosystem metabolism and its components; (2) stream metabolic response over gradients of space, time, and disturbance severity; and, (3) how all of the above is mediated by stream and watershed geomorphology. We ask: 1) What are the relative effects of fire disturbance severity, and watershed geomorphic characteristics on stream metabolism? 2) Do the respective effect sizes of disturbance and stream geomorphology on response variables change when we investigate them at different spatial scales? 3) What spatial scale—watershed, riparian buffer across the stream network, stream segment, or stream reach—is most relevant for quantifying wildfire effects on stream metabolism? and, 4) What are the drivers (light vs. nutrients) of stream metabolism in these fire-affected systems?

Methods

Study system and sites

Our investigation took place in the Big Creek watershed, part of the Salmon River basin in central Idaho (Figure 1;-114.738996 E, -115.466110 W, 45.290705 N, 44.882592 S). In this semi-arid region, late-summer wildfire is an important and frequent part of the local disturbance regime; several large fires in the past two decades have created a mosaic of disturbance across the landscape, providing a natural laboratory to investigate the impacts of fire disturbance on ecosystem metabolism. Our sampling areas lay on a boundary between Hot Dry Canyons and Southern Forested Mountains of US EPA (2014) Level IV Ecoregions (available online at http://www.epa.gov/wed/pages/ecoregions/level_iii_iv.htm#Level IV). Geological parent materials were derived from the granitic Idaho Batholith. Annual precipitation in the watershed is approximately 40 cm, with the majority falling as snow (Minshall 2003); stream flows are driven by snowmelt in late spring and early summer (May and June), with base flows occurring from July to September.

Plant assemblages in all watersheds were similar, with upland vegetation dominated by subalpine fir (*Abies lasiocarpa* Hook. Nutt.), Douglas-fir (*Pseudotsuga menziesii* Mirb. Franco) and Engelmann spruce (*Picea engelmannii* Parry ex Engelm.) at higher elevations and on north-facing slopes, and by ponderosa pine (*Pinus ponderosa* C. Lawson) and sagebrush (*Artemisia tridentate* Nutt.)-grass communities on south-facing slopes (Jackson and Sullivan 2009). Riparian forests were characterized by gray alder (*Alnus incana* L. Moench), red osier dogwood (*Cornus sericea* L. ssp. sericea), Rocky Mountain maple (*Acer glabrum* Torr.), willow (*Salix sp.* L), thimbleberry (*Rubus parvifloris*), mallow ninebark (*Physocarpus malvaceus*) and water birch (*Betula occidentalis* Hook.) (Jackson and Sullivan 2009).

Big Creek is largely confined to the Frank Church-River of No Return Wilderness. The degree of anthropogenic influence on this 13,000-km^2 roadless area is low. Historical fire

regimes for *Pseudotsuga*-dominated mixed conifer forests are highly variable in severity and frequency (Agee 1993), and estimates of the historical fire return interval in this region are inconsistent, ranging from 13 (Heyerdahl et al. 2008) to 80 years (Pierce et al. 2004). Since 1985, wildland fires within the wilderness have been primarily managed for resource benefits (e.g., forest health). Portions of many watersheds within the Big Creek drainage burned in 1988, 2000, 2005, 2006, 2007 and 2008 wildfires. Of special note is the Diamond Peak wildfire complex, which burned 606.1 km^2 of the Big Creek and Middle Fork Salmon River drainages in August and September 2000. This fire is unique in its extent, providing multiple burned stream reaches that all experienced fire at the same time but vary in stream characteristics and burn severity and extent.

We monitored 18 tributaries of the Big Creek watershed in July and August of 2013. These 18 tributaries encompassed a range of stream orders (2^{nd} to 6^{th} order) and watershed sizes (325506.9 km^2 to 4993.0 km^2). Tributary sites were also selected to encompass watersheds that had a range of burn severities and time since last burn (6 to 30 years). Sixteen sites were independent tributaries, while two (North Fork Cabin Creek and Cow Creek) were sub-watersheds nested inside a larger tributary watershed (Cabin Creek). These sub-watersheds were treated as spatially independent because of their considerable physical distance from one another, and the fact that they contributed less than 10% to the discharge of the main-stem river below their outlets. All tributary sites were located within 1 km of the tributary outflow into Big Creek (Figure 1).

Stream metabolism measurements

Stream metabolism was measured in the Big Creek watershed during summer base flows after spring snowmelt had subsided. Dissolved oxygen concentration ($[O_2]$) and water

temperature were monitored at each station at 10-minute intervals using a Yellow Springs Instruments (YSI) 6600 V2 sonde equipped with an optical dissolved oxygen (ROx) sensor. Sondes were deployed to a site for 3-8 days at a time. Sondes were calibrated using an air-saturated water procedure at the beginning of the field season. To ensure that the oxygen sensor calibrations had not drifted over time, all sondes were recalibrated if needed after being placed in a stream together for 12-24 hours once a week throughout the field season. Sensor [O_2] measurements were calibrated to [O_2] measurements on a subset of samples as determined by Winkler titrations at the time of sonde deployment and retrieval. Winkler samples were collected and titrated on a Dosimat following the basic methods of the Marine Chemistry Laboratory at the University of Washington (available online at http://www.ocean.washington.edu/file/Sampling+Procedures).

Light intensity, recorded in units of lumens ft^{-2}, was logged at each site at 10-minute intervals using a HOBO® Pendant (Onset Computer Corporation, Bourne, MA, USA) light logger deployed on the streambank near the metabolism monitoring site but outside the vegetated zone. Site-specific light data was converted from lumens ft^{-2} to PAR, measured in units of microeinsteins m^{-1} s^{-1}, using a regression equation in R (R Development Core Team, 2014). To assess the degree of riparian shading on each individual stream, we also completed upstream transects of 0.5-1.5 km with a HOBO ®Pendant, measuring every second to characterize the average irradiance reaching the stream surface along the thalweg. These data were used as a proxy for existing riparian cover and recovery since burn by calculating a "shading ratio" of average riparian light measured in the transect to average light measured at the static light meter (outside the directly shaded riparian area). A higher shading ratio is indicative of less available light.

Environmental data

Hydrologic flow was measured at each site using a Marsh-McBirney flowmeter (Hach Company, Loveland, CO, USA): at least 20 samples of velocity (at 60% of total depth) and depth were measured across a cross-channel transect, and discharge was subsequently calculated. The channel was characterized for about 1-2 km upstream of the monitoring station using 10-20 width and depth measurements, spaced about 100 m apart from one another.

Water samples for total nitrogen (TN), total phosphorus (TP), dissolved organic C (DOC), phosphate (PO_4^{3-}), nitrate (NO_3^-), nitrite (NO_2^-), ammonium (NH_4^+), and silicate (SiO_4^{2-}) were collected from each stream at the time of sonde deployment, filtered and/or acidified in the field, and frozen or refrigerated as soon as possible after collection; all samples were analyzed by the Marine Chemistry Laboratory at the University of Washington. TN was determined using perchloric acid digestion followed by analysis with automated colorimetry. TP concentration was determined colorimetrically after persulfate digestion and reaction with molybdate and stannous chloride (Valderrama 1981). All other nutrients ($[NO_3^-]$ $[PO_4^{3-}]$,$[NO_2^-]$, $[NH_4^+]$ and $[SiO_4^{2-}]$) were determined following the protocols of the WOCE Hydrographic Program using a Technicon AAII System (UNESCO 1994). Samples for DOC analysis were acidified to pH 2 with hydrochloric acid immediately after collection; all nutrient and DOC samples were frozen until analysis on a Shimadzu TOC-Vcsh DOC analyzer (Shimadzu, Kyoto, Japan) (UNESCO 1994).

Estimates of stream periphyton biomass were obtained by scrubbing six rocks per stream (the primary algal substrate in these streams). Six rocks were collected at random throughout the upstream transect to characterize the stream channel; though rocks were selected in random locations, we attempted to select rocks that were of an "average" size for the reach. We

quantified chlorophyll *a* content per unit rock surface area via fluorimetry after extraction in methanol as described in Holtgrieve et al. (2010).

GIS methods

To characterize burn severity for each watershed of interest, we obtained remotely-sensed burn severity data for every fire larger than 20 ha^2 in the Big Creek Watershed from the Aldo Leopold Wilderness Research Institute, Rocky Mountain Research Station (Parks et al. 2014a). Raster data are available from 1972 to 2012, but we chose to only use data dating back to 1984, when LANDSAT imagery was first used to map fires. We used the Relativized Burn Ratio (RBR) rather than the more commonly used differenced Normalized Burn Ratio (dNBR) metric to measure burn severity. RBR is a more accurate burn severity metric in areas that are characterized by brush and shrubs (such the Big Creek watershed, which is sagebrush-steppe over much of its lower and mid elevations) rather than tall forest, because it can detect change in shrub cover as well as tree cover after a fire (Parks et al. 2014a).

RBR is continuous data, but for ease of analysis, we re-classified the data using the classification system developed by Parks et al. (2014a) for the Northern Rockies. Fire severities within the extent of mapped fires were classified as follows: Very Low/Unburned, Low, Moderate, and Severe. All other area within a watershed of interest was classified as Unburned since 1984 (though it should be noted that there are several major known areas that burned within the Big Creek watershed prior to 1984, but these fires were not mapped using remote sensing).

Using ArcGIS (Environmental Systems Resource Institute 2011), we used the Hydrology toolset in ArcMap's Spatial Analyst toolbox to delineate watersheds of interest within the Big Creek watershed from a digital elevation model (DEM) of the area (available online from the

National Elevation Dataset at http://ned.usgs.gov/). The delineated watershed polygons were used to estimate total watershed area, then to clip out the RBR data for all fires for each watershed of interest; these fires were then stitched together using Arc's Mosaic tool. For areas that had burned more than once within a watershed, when we executed the Mosaic tool, we specified that each area that had two or more fires overlapping should take on the values for whichever cells had higher RBR numbers (i.e., more severe ratings). We did this because the severity of a burn can affect the severity of future burns, with the highest severity fires having the strongest effect (Parks et al. 2014b). Furthermore, it has been demonstrated in the Big Creek watershed that high severity burns have the strongest effect on riparian conditions, and therefore presumably on stream ecosystems (Jackson and Sullivan 2009, Arkle and Pilliod 2010, Jackson et al. 2012). Zonal statistics were used to calculate the total area burned per watershed of interest, in addition to the percent area burned within each severity class. Slope rasters were generated from the DEM and used to calculate average slope (degrees) for each watershed of interest.

Because we were interested in examining the effects of fire at various spatial scales, and determining which scale (if any) had the strongest effect on stream metabolism, we also generated data for burn severity and watershed characteristics at nine smaller scales: 1) a riparian forest buffer extending throughout the entire watershed's stream network; and 2)-9) riparian forest buffers extending 4000, 3500, 3000, 2500, 2000, 1500, 1000, and 500 m upstream from the study site, respectively. Riparian forest buffers were defined as an area within 20 m of the stream bank, following several previous ground-truthed studies of fire and riparian areas in the Big Creek watershed, which found that even for large-order streams, the vegetated area of the riparian zone did not extend more than about 20 m beyond the stream (Jackson and Sullivan 2009, Jackson et al. 2012, Arkle 2014). A polygon layer of active channel stream width was

derived from the NetMap stream layer data (Benda et al. 2007), which is available online at www.terrainworks.com. A 20-m buffer was created around this polygon using ArcMap tools, and a subsequent Erase operation removed the stream width polygon. The resulting buffer layer, which covers the entire riparian forest of each watershed of interest, was used to clip out burned areas from the burn severity rasters; area burned and percent area burned per severity class were calculated from the clipped buffer zone using the same method used for the whole-watershed analysis. These riparian buffers were used to clip out slope rasters and calculate average slope within the riparian buffer zone for each stream network.

Similarly, we created riparian buffer zones of various lengths upstream from the study sites, in order to determine the degree of downstream influence (if any) of upstream disturbance history and/or watershed characteristics. To do this, we used the Network Analyst and Linear Referencing toolboxes in ArcMap to create routes along the lengths of each stream, extending 4 km upstream of each study site. After building event tables for each route, event feature layers were created for each route and the events (located every 500 m along the route from 0 to 4 km) exported as point feature layers. These points were used to split the original routes at each 500 m interval, and the resulting line segments (extending upstream 500, 1000, 1500, 2000, 2500, 3000, 3500, and 4000 m of the study sites, respectively) were used to clip out accurately measured segments of the previously created network riparian buffers by executing the Intersect tool. Each set of resulting short riparian buffer polygons were then used to clip out burn severity and slope data for each stream, as described above.

Metabolism modeling

We estimated rates of gross primary production (GPP), ecosystem respiration (ER), and gas exchange (G) by fitting a mass-balance model describing dissolved oxygen dynamics and the

stream [O_2], temperature and light data (Bayesian Metabolic Model, or "BaMM"; as described in Holtgrieve et al. 2010). The model accounts for dissolved oxygen concentrations as determined by production via photosynthesis, consumption via respiration, and exchange between the stream and the atmosphere (Holtgrieve et al. 2010),

Equation 1. $$\frac{dO_2}{dt} = \left[k\left(\left[O_{2,sat}\right] - [O_2]\right) - R + P\right]/D$$

where $[O_2]$ is the dissolved oxygen concentration (mg m^{-3}), $[O_{2,sat}]$ is the dissolved oxygen concentration at atmospheric equilibrium, R is the instantaneous respiration rate, P is the instantaneous rate of photosynthesis (both in units of mg O_2 m^{-2} h^{-1}), and D is the average mixed layer depth (m). The first term in the above equation is the net effect of gas exchange, which is the gas transfer velocity, k, times the O_2 concentration gradient. In this model, photosynthesis is modeled as an asymptotic function of light intensity, respiration is a positive function of water temperature, and gas exchange depends on the concentration gradient between the stream and the atmosphere, and the re-aeration coefficient.

We then used an adapted version of this basic model in order account for variability in the carbon substrate supporting heterotrophic respiration (Schindler et al., in prep) and different sensitivities to temperature (Jankowski et al. 2014). This revised model considers the potential for two substrate pools to support R: respiration of ambient carbon substrates or "background R", R_b, and heterotrophic R based on substrates derived from primary production in recent time, R_p,:

Equation 2. $$R_{total}(T,t) = R_b(T,t) + R_p(T,t)$$

R_b was formulated as follows:

Equation 3. $$R_b\ (T,t) = R_b(T_{ref}) * e^{-E*(T-T_{ref})/kTT_{ref}}$$

R_b was estimated at each time step as a function of the measured stream temperature (T_{ref}, the reference temperature, was set to 20°C). R_p was considered a lagged function of

photosynthesis; in other words, we assumed that organic substrates produced by some portion of *n* previous time steps of photosynthesis was directly consumed and respired by heterotrophs. To do so, we estimated an α parameter, which is the slope of a linear function that describes how much of the average of the six previous time steps (the past hour) of photosynthesis is respired. The greater the value of this slope parameter, the higher the influence of photosynthetically-derived carbon on the rate of ER.

R_p was formulated as follows for the 'previous timestep' lag function:

$$\text{Equation 4. } R_p\ (T,t) = \exp\left(-\frac{E_p}{kT}\right) * (\alpha_i) * P[I(t-1)]$$

R_p was formulated as follows for the 'weighted average' lag function:

$$\text{Equation 5. } R_p\ (T,t) = \frac{((3*\exp\left(-\frac{E_p}{kT}\right)*(\alpha_i)*P[I(t)])+(2*\exp\left(-\frac{E_p}{kT}\right)*(\alpha_i)*P[I(t-1)])+\exp\left(-\frac{E_p}{kT}\right)*(\alpha_i)*P[I(t-2)])}{6}$$

In this analysis, when allowing for a temperature dependent *R*, we fixed E_v and E_b at the temperature sensitivity values expected for heterotrophic respiration (E_v=0.65, E_b=0.32) (Allen et al. 2005).

For each stream, we estimated metabolism parameters, including R_b, α, *k20*, $\alpha P(I)$, P_{max}, O_{start}, and σ, for a set of potential respiration models (Table 2), focusing on the three most relevant:

1) temperature-sensitive ER using only one carbon substrate (R_b only), using the following simple formulation for R_b (T,t):

$$\text{Equation 6. } R_b\ (T,t) = R_b * 1.047^{(T(t)-20)}$$

2) Two-source, temperature-sensitive ER (R_b and R_p) using photosynthesis from the previous timestep (Equation 4) and Equation 3 for R_b; and,

3) Two-source ER using a weighted average of the previous 30 minutes of estimated photosynthesis (Equation 5). Models were fit to the data using maximum likelihood, using the

Solver function in Excel. Models were compared and the best model selected using AIC_c (Burnham and Anderson 1998, Burnham et al. 1998, Anderson and Burnham 2002).

Statistics

All multivariate statistics and linear modeling was done in R (R Development Core Team 2012). We used principal component analysis (PCA) in the vegan and pastecs libraries in R to summarize variation among streams in their disturbance history, chemical, and geomorphic/physical conditions. Before analysis, all variables were transformed appropriately to meet assumptions of normality. The first PCA (PCA_{chem}) summarized variation in stream chemistry and light conditions among streams; variables included shading ratio, DOC, TN, TP, PO_4^{3-}, SiO_4^{2-}, NO_3^-, NO_2^-, NH_4^+, TN:TP, and average chlorophyll-a. The second PCA (PCA_{ws}) summarized variation in stream disturbance history and watershed geomorphic data; variables included average watershed slope, watershed area, average depth, average width, stream discharge, percent area burned, percent burned VERY LOW, percent burned LOW, percent burned MODERATE, and percent burned SEVERE. Axis and vector significance were determined by Monte Carlo analysis with 1000 random permutations. We regressed the resulting composite axes (principal components 1 and 2) from PCA_{chem} against PCA_{ws} to evaluate how variation in stream chemistry and light co-varied with disturbance history and watershed geomorphic characteristics. In addition, we used the axes of these PCAs in principal component regressions to evaluate how variation among stream metabolic condition and its components (GPP and ER) was explained by composite variation in stream chemistry/light or disturbance history/watershed geomorphology.

To evaluate the effect of scale, we repeated these analyses for each of the 10 scales at which we evaluated disturbance history and watershed geomorphic variables (watershed scale;

network-scale riparian forest; and riparian buffers at reach lengths of 500, 1000, 1500, 2000, 2500, 3000, 3500 and 4000 m upstream from the study site).

To parse the unique effects of different sets of explanatory variables, we used partial redundancy analysis (pRDA). pRDA is a multivariate approach to identify the unique effect of one set of explanatory variables (such as geomorphology or disturbance history) on a set of response variables, while removing the effect of other sets of explanatory variables. pRDA can also be used to determine how much variance in the response matrix is due to a joint (confounded) effect of groups of variables, and how much variance is explained (constrained) vs. residual (unconstrained). We performed pRDA at each of the 10 scales described previously.

We evaluated the influence of disturbance history, watershed geomorphology and stream environmental conditions on stream metabolism by regressing our estimated P:R, GPP, and R_t values from the metabolism model described above against watershed geomorphic, disturbance history, and stream chemistry variables. We repeated the linear modeling for each of the 10 spatial scales at which we wished to evaluate the potential effects of disturbance on stream metabolism. Models to compare effects at each scale were fit by maximum likelihood and compared with AIC_c.

For each of ten scales, we calculated the effect sizes for PC1 and PC2 of the linear models that included the variables PC1+PC2 by dividing the regression coefficient by the standard error of the regression coefficient.

Results

Watershed geomorphology and burn history

The first axis of the watershed PCA ($PC1_{ws}$) captured differences among streams in geomorphic variables, primarily watershed size, slope, and stream discharge, whereas the second

PCA axis ($PC2_{ws}$) captured differences in watershed burn history, primarily percent area burned and the severity of the burn (Figure 2, Table 1). We found that the percent of variation among streams attributed to the first and second axes of the geomorphic/burn history PCA varied with the spatial scale of analysis (Figure 3, Table 1). At coarse scales (i.e., watershed-scale and network-riparian scale) geomorphology accounted for most of the variation among streams, while at finer scales, burn history accounted for most of the variation we observed. At coarse scales, $PC2_{ws}$ (burn history) was not a significant axis and there was only one significant gradient in the data; in other words, at coarse scales, burn history was strongly correlated with watershed geomorphology. At finer scales (e.g., $\leq$ 4000m), $PC2_{ws}$ became significant and orthogonal to $PC1_{ws}$; i.e., at finer scales, burn history was independent of local geomorphology (Appendix 1: Supplemental Figures 1a-j).

Percent of the stream network riparian buffer that had burned was strongly correlated with the percent of total watershed burned (linear regression, r^2=0.998, F=7145, df=17, p<0.001). Similarly, percent of total watershed burned also significantly predicted the percent of the riparian network that had burned with high severity (r^2=0.728, F=45.46, df=17, p<0.001) and the percent of the whole watershed that had burned with high severity (r^2=0.807, F=71.23, df=17, p<0.001) (Figure 4). However, at finer scales, percent total watershed burned was not correlated with percent riparian burn (Table 2a) or percent riparian burn with high severity (Table 2b) as well, and in some cases was not a significant predictor, although there was a clear trend towards stronger relationships at coarser spatial resolution (Supplemental Figures 2a-h).

Effects of geomorphology and burn history on stream chemistry and light conditions

Streams in the Big Creek watershed varied substantially in physical and chemical conditions (Table 3). For example, total nitrogen concentration (TN) varied between 79.4 and

457.9 µg L^{-1}, total phosphorus (TP) between 3.80 and 9.50 µg L^{-1}, and average stream width between 0.9 and 23.6 m. We found that light, nitrogen, and phosphorus were the variables that best explained differences among streams; first axis of the stream chemistry and light PCA ($PC1_{chem}$) primarily captured differences among streams in the degree of shading and in nitrogen concentration (35.1% of variation) whereas the second axis of this analysis ($PC2_{chem}$) captured differences in phosphorus concentration (23.4% of variation; Figure 5, Table 1).

Principal component (PC) regressions between watershed characteristics and stream co nditions demonstrated that chemistry and light variables ($PC1_{chem}$ and $PC2_{chem}$) varied predictabl y with both $PC1_{ws}$ and $PC2_{ws}$ (Table 4). Specifically, $PC1_{chem}$ (light and nitrogen concentration) was significantly, negatively correlated with $PC1_{ws}$ (geomorphology) at all ten scales of analysis (Figure 6a-b; see Supplemental Figure 3a-j to view all scales; Table 4): the smaller and steeper th e watershed, the less light and higher nitrogen concentration it had.

Stream metabolism and stream chemistry

We were able to estimate GPP, R_t and G based on *in situ* observations of diel changes in oxygen concentrations for 13 of 18 streams in the study. In five streams we were unable to fit a respiration model; these streams were extremely production-dominated and had large gas exchange rates for which no respiration model could be fit. In other words, R_t was less than G so could not be estimated (Table 5). We designate these five streams 'superautotrophic' and leave them out of subsequent calculations that required estimates of respiration rates (e.g., P:R ratios).

For the 13 streams where respiration could be estimated, the ratio of R_p (respiration derived from photosynthetic carbon) to R_b (base respiration based on background carbon) was high (average =7.8), ranging from 0.72 to 38.2; in four of these 13 streams, > 99% of the respiration was derived from photosynthesis in recent time steps. Regression of R_t against GPP

for all streams where R_t could be estimated indicated that respiration is supported primarily by production in these steep, low-DOC mountainous streams (r^2=0.399, F=7.968, df=12, p=0.015, β_1=0.87).

Stream nitrogen concentration and riparian shading ($PC1_{chem}$), which was previously de monstrated to correlate strongly with stream geomorphology ($PC1_{ws}$) were significantly, negative ly correlated with the log of GPP (r^2=0.382, F=9.884, df=16, p=0.006), i.e., streams with less sha ding and lower TN were more productive, whereas streams with more shading and higher TN we re less productive. Stream nitrogen concentration and riparian shading were also negatively corre lated with log(P:R), indicating that streams with more shading and more TN tended toward heter otrophy) but this relationship was not statistically significant (linear regression: r^2=0.139, F=1.77 1, df=11, p=0.210) (Figures 7 and 8, Table 4).

$PC2_{chem}$ (phosphorus concentration) and log(R_t)were significantly, positively correlated (r^2=0.463, F=9.471, df=11, p=0.01) (Figure 9, Table 4); log(P:R) was negatively correlated with $PC2_{chem}$. Both of these relationships indicate that streams became more heterotrophic with increasing P concentrations, although this relationship was marginally significant in the case of log(P:R) (r^2=0.238, F=3.436, df=11, p=0.09).

Together, these results link stream metabolic condition to a combination of stream size and post-disturbance riparian recovery, which controlled the light and chemical conditions of those streams. Severely burned streams tended to be highly shaded, as shown in the PC regression which linked small stream size with low light and high nitrogen. These streams, due to their low light conditions, had low GPP and also low respiration, but were overall heterotrophic; they cluster together on both PCA_{ws} and PCA_{chem}. In contrast, larger and less severely burned streams tended to not be as heavily shaded. Due to their higher light conditions,

large, lightly burned streams had much higher production (and in many cases higher respiration), and overall they tended to be autotrophic or superautotrophic (Figure 2, Appendix 1: Supplemental Figure 1a-j, Figure 6).

Spatial variation in effects of burn history and stream geomorphology on stream metabolism

Watershed geomorphology and burn history were significantly associated with metabolic properties of streams but the strength of these relationships changed with the spatial scale of the analysis. Multiple regressions showed that, for most scales, GPP was best explained by a combination of stream geomorphology and burn history, with smaller/steeper and more severely burned streams having lower productivity. The best-fit models included both stream geomorphology ($PC1_{ws}$) and burn history ($PC2_{ws}$), except for the 500 m riparian buffer scale, which only included $PC1_{ws}$, and the 3.5 km riparian buffer scale, which also included $PC3_{ws}$ (Table 6a). Respiration, in contrast, was best explained solely by stream geomorphology for most spatial scales, with larger and more open streams having higher respiration. Best-fit models included only stream geomorphology ($PC1_{ws}$), except for network riparian scale which included only burn history ($PC2_{ws}$) (Table 6b). The ratio of productivity to respiration (P:R) was best explained by stream geomorphology at a coarse spatial scale. At a finer spatial scale, P:R was best explained by burn history; for all scales ≤4000m, best models included $PC2_{ws}$ and in a few cases $PC3_{ws}$ (Table 6c).

In addition, the effect of stream geomorphology and burn history on stream metabolic conditions changed with spatial scale. Stream geomorphology ($PC1_{ws}$) had a strong, significant effect on GPP at all spatial scales considered, although effect size did increase at finer spatial scales (i.e., stream geomorphology had the strongest effect on GPP at the finest spatial scale; Spearman's rho=0.76, p=0.01) (Figure 10a). Burn history ($PC2_{ws}$) had a smaller effect size than

stream geomorphology across all spatial scales, but the magnitude of the effect changed much more from fine to coarse scale. Burn history had the weakest effect on GPP at a fine scale, and much stronger effects at coarser spatial scale, nearly matching the strength of stream geomorphic effect. This correlation with scale was highly significant (Spearman's rho=0.81, p=0.007). In sum, for GPP, effect size for $PC1_{ws}$ and $PC2_{ws}$ was divergent at finer scales, converging to nearly the same magnitude at coarser scales.

A similar pattern was observed for respiration, where the effect sizes of geomorphology and burn history were divergent at finer scales but converged to similar magnitudes at coarse spatial scales (Figure 10b). Stream geomorphology ($PC1_{ws}$) effect on R_t was strongest at fine spatial scales, weakening over increasingly coarser scales; effect size's correlation with scale was significant (Spearman's rho=0.73, p=0.01). Burn history ($PC2_{ws}$) effects on R_t were weak at fine scales but increased to match the magnitude of $PC1_{ws}$'s effect size at the watershed scale. Burn history's effect size correlation with scale was visually suggestive, but only marginally significant (Spearman's rho=0.455, p=0.19). Interestingly, the effect of burn history on R_t was positive in direction at finer spatial scales, and negative at coarser scales—i.e., at fine scales more burn resulted in more respiration, while at coarse scales more burn did not result in more respiration— while the effect of burn history on GPP did not change in direction with varying scale. Effect size of geomorphology and burn history on P:R were not significantly correlated with scale for either $PC1_{ws}$ (Spearman's rho=0.09, p=0.81) or $PC2_{ws}$ (Spearman's rho=0.05, p=0.89) (Figure 10c).

Variation in stream chemistry, light and metabolism explained by burn history vs. geomorphology

We used a partial redundancy analysis (pRDA) to complement the more traditional linear regressions described above. While multiple linear regression and subsequent model comparisons quantify which combination of explanatory variables best predict a given response, and describe the magnitude and direction of the effect of each explanatory variable on the response, a pRDA gives a more conceptual overview of how the explanatory and response variables relate to one another. The pRDA parses how much variation in the response variables can be explained, how much of the explained variation in the response variable can be attributed to each explanatory variable, and how much of the variation is confounded. Complete results of our pRDA can be found in Tables 7a-c.

Results of the pRDA showed that more variance in stream chemistry, riparian shading, and metabolic components was explained by burn history and geomorphology at finer scales than at coarser ones (Figure 11, Table 7a). In a pRDA, the components represent single exclusive (non-overlapping) partitions of response variance, such as would be represented in a Venn diagram. Results for the components indicated that: more variation in chemical and metabolic conditions was explained at fine scales than at coarse ones; confounded variation was greater at coarser scales than at finer ones; variance explained by geomorphology was fairly consistent between scales; variance explained by wildfire disturbance increased from coarse to fine scales; and variance explained by geomorphology was greater than that explained by fire or by confounded variance (Table 7b). It should be noted that most of the p-values for the components (Table 7b) are marginally significant, while the marginal effects (Table 7c) were generally significant. However, because of the high percent of variation explained by the components, we regard these results as ecologically meaningful.

Marginal effects in a pRDA represent variance attributable to single explanatory data sets (i.e., just fire, or just geomorphology) without partialling out any others: they include the confounding variance that cannot be separated, or the overlapping parts of the Venn diagram. Marginal effects can be construed as the effect size (relative to total variance or explained variance) of the explanatory matrices. Results for marginal effects in our pRDA indicated that the relative effect size of geomorphology decreased slightly at finer scales of analysis, while the relative effect size of burn history increased slightly at finer scales of analysis. Overall, the relative effect size of geomorphology was consistently larger than that of burn history across scales (Table 7c).

Discussion

Our results demonstrate that stream metabolic condition is sensitive to a combination of stream size/geomorphology and post-disturbance riparian recovery, but that the strength of these relationships changed with the spatial resolution of the analysis, with a general trend that finer spatial resolutions had stronger correlations. Light is the primary mechanism driving stream metabolism, controlled by riparian succession and mediated by stream size, whereas nutrients played a secondary role in stream metabolic condition.

We propose an update and amendment to the Gresswell conceptual model of a stream's post-fire response through time that takes into account the geomorphic context and burn history of streams. Instead of a slow fading of the initial fire pulse reaction over decades, we observed a relatively rapid (within 6-12 years of last burn) and pronounced downward shift in incident radiation due to rapid riparian regrowth, and concomitant drop in stream GPP and autotrophic metabolism. The 'classic' disturbance response, which presents one idealized stream over a time continuum, is actually highly mediated by the spatial resolution of analysis and by local stream

geomorphology. Arkle et al. (2010) showed that post-fire response in temperature tends to be rapid and extreme in small, severely burned streams—from much warmer than unburned streams in the early post-fire years to much colder than unburned streams after riparian regrowth— in comparison to the gentle and moderate response proposed by the Gresswell model.

We showed that light was a primary driving variable for stream metabolic response to fire. Thus, the presence or absence of riparian vegetation (and the speed and manner of its recovery) will be the limiting factor in stream metabolic/productivity recovery from disturbance. In other words, the pattern in stream productivity recovery from fire is tightly linked to riparian succession (Dwire and Kauffman 2003, Pettit and Naiman 2007). We found that the recovery of the riparian forest was linked to network position and stream geomorphic setting, however. Therefore, to understand post-fire recovery in productivity, it is important to consider the geomorphic setting of your system. Variability in post-fire riparian response trajectories could depend on many factors including aspect, species, soil moisture, or fire severity or more complex variables such as the cascading and interactive effects of climate change, an altered fire regime, and subsequent drastically decreased seedling recruitment.

We also found that nutrients appear to play a secondary role in stream metabolism in tributaries to Big Creek. Nutrients could become more of a driving force in metabolism during times of year when the upland is more hydrologically connected to the stream (e.g., during the rainy seasons of spring and fall). If this is the case, then the degree of upland (as opposed to riparian) fire disturbance and the way it changes soil nutrient cycling, erosion, and runoff would become more important in predicting stream metabolism during those seasons. During the summer low-flow season when our observations were made, there is likely very little hydrological connectivity between the upland and the stream (with the exception of during and

after rare summer thunderstorms and potentially some groundwater connectivity). During this time, local conditions and past disturbance history in the riparian zone are likely to have a disproportionate impact on stream metabolism compared to upland conditions and past disturbance history.

Our results suggest that stream succession proceeds along a trajectory that depends heavily on the attributes of the system in question and cannot necessarily be generalized among biomes or even among stream orders in the same ecosystem. For example, Betts and Jones (2009) worked in boreal forest where post-fire changes in metabolism were strongly linked to fire's ability to melt permafrost, alter hydrological connectivity and microbial activity, and release soil nutrients into the streams, whereas we worked in sub-alpine and sage-steppe systems with no permafrost. Betts and Jones observed elevated GPP and respiration in burned streams (whereas we observed decreased GPP and respiration in small burned streams but normal/elevated GPP and respiration in large burned streams), but their streams were in the very early stages of post-fire succession, and likely experiencing a 'fire pulse' effect driven partially by increased PAR and partially by elevated N and SRP.

By contrast, working in systems very similar in climate, vegetation regime, and fire regime to our systems, Tuckett (2007) found no difference in metabolism between unburned streams and streams burned between two and 11 years ago, but noted persistent, elevated GPP in burned and scoured streams. Burned and scoured streams in which riparian vegetation is unable to reestablish due to fire-induced bank instability and annual scouring floods and debris flows experience a sort of persistent 'fire pulse' effect and do not proceed along a 'normal' succession trajectory to pre-burn conditions. Other authors, such as Arkle et al. (2010), Harris (2013),

Dunham et al. (2007) and Rosenberger et al. (2011) have also noted that fire effects seem to be strongest and most persistent in these burned and scoured streams.

Most tributaries to Big Creek included in our study are not prone to scour and debris flow, and therefore our study streams did not experience delayed succession or a permanent state of 'fire pulse.' However, there is one exception: Canyon Creek, among the smallest and steepest of our watersheds, with nearly 100% of its riparian zone burned in 2008, did not follow the pattern of succession seen in other small, steep and severely burned streams: rapid riparian recovery driving very low light, low GPP, and heterotrophy. By contrast, Canyon Creek had the highest P:R ratio of any stream (21.03) and the highest levels of chl-a; for its size and mean width, it had comparatively more light (meaning less riparian regrowth) than other streams of similar size and burn history. All of these observations, in addition to our field observation that Canyon Creek appeared to have very high levels of bank instability and incision compared to most of the other streams, indicate that this stream may still be undergoing post-burn erosion and scouring during high flows, leading to its unusually elevated metabolism and delayed riparian succession.

We observed a relationship between low light and high concentrations of nitrogen in small, heterotrophic streams. High nitrogen concentrations are commonly observed in streams during the first 1-2 years post-fire (Bayley et al. 1992, Hauer and Spencer 1998) due in part to increased microbial or thermal decomposition of vegetation and soil organic matter or decreased microbial competition with vegetation for ammonium and increased nitrification (Betts and Jones 2009). However, the streams in which we observed high nitrogen concentrations were long past the response window in which elevated nitrogen is usually observed (6-12 years post-fire), and it is likely that their elevated N is due to different drivers than those described by Bayley et

al. and Hauer and Spencer. We speculate that our observations of elevated N could be for several reasons: rapid and dense regrowth of N-fixing species such as alder (Compton et al. 2003); increased N-fixing algae present in these streams post-disturbance (Baxter 2014); and higher detectability of the above two possible effects because of a comparatively low discharge in small streams. Large streams, by contrast, likely experience the same or even greater inputs, but the effects are diluted in their much larger discharges.

Our model was unable to estimate respiration in five out of 18 streams. We assume that these streams do have some respiration. However, their extremely high rates gas exchange masked the comparatively small rates of respiration, which must have been equal to or less than the rate of gas exchange in each of these streams. These five streams happened to be the five largest-order streams in the study, with high discharge, but still had steep stream gradients, likely contributing to their high *G*.

We found that long-term post-fire effects on the metabolism of large, wide streams are less detectable: the effects of rapid riparian regrowth (shading, elevated N) are small in comparison to the effects of local geomorphology. In contrast, long- term successional effects in a small, narrow stream are highly detectable because rapid riparian regrowth can readily shade out the channel. Perhaps over the very long term, if the non-riparian forest canopy returns and provides additional shade to large streams or outcompetes the dense riparian vegetation in small streams, the dampened production seen in small streams will approach that in larger streams.

We found that burn history is collinear with watershed geomorphology at coarse spatial resolutions (whole-watershed and network riparian scale), but that at medium to fine spatial resolutions (4000 m riparian buffer and smaller) the watershed geomorphology becomes decoupled from disturbance history. This is likely due to simple probability, because small

watersheds are likelier to have been burned in their entirety over the last 30 years of our fire data. Steep watersheds are also likely to burn more quickly, severely, and over more of their area (Finney et al. 2010).

We found that, at a whole-watershed and network riparian scale, total percent burned does an excellent job of predicting percent burned with high severity and percent riparian burned. Arkle and Piliod (2010), whose work in Big Creek clearly demonstrates the dual importance of fire severity and whether the fire occurred in the riparian zone, used this predictive relationship to argue that using such a 'lumped' larger-scale metric was an adequate proxy to predict fire effects at a finer scale, e.g., on riparian zones. However, we show that this relationship weakens and eventually breaks down at finer spatial scales. We therefore caution that, if researchers are interested in investigating fire disturbance impacts at a segment- or reach-scale, to use the appropriate spatial resolution of data. Percent of watershed burned at high severity does not necessarily predict percent of riparian burned at high severity over, for example, a 500-m stream reach.

We found that the smaller and steeper the watershed, the more shaded and more elevated the stream's nitrogen concentration. GPP, which is driven in these systems by light, also showed a strong relationship with watershed geomorphology, with small, steep watersheds (which happen to be severely burned) being much less productive. This relationship was strongest at finer scales, where a small change in stream geomorphology produced a larger change in GPP. This is likely because at coarse spatial scales, small changes in geomorphology averaged over the whole watershed do not predict the relevant local conditions driving GPP (light).

Respiration, conversely, was not linked strongly to burn history, geomorphology, light, or nitrogen concentration, but rather to stream phosphorus concentration. Although phosphorus

correlation with respiration is not a new observation in freshwater ecology (Ramirez et al. 2003), this is somewhat surprising because we showed that most respiration in these low-DOC streams is linked to GPP and our model showed overall low rates of 'background' respiration (respiration not based on photosynthetically produced carbon). Our observations suggest a phosphorus limitation in some of these streams. Similar to Tuckett's work in Idaho streams, respiration varied much more among study streams and did not show clear patterns, unlike GPP. This variability in respiration probably explains the corollary lack of strong relationship between P:R and environmental variables. Phosphorus in tributaries to Big Creek is linked to geology (Davis and Minshall 1999); tributaries just hundreds of meters apart from one another (e.g., Cliff Creek and Pioneer Creek) flow over distinctly different rock formations (e.g., Idaho Batholith vs. metamorphic quartz), and therefore often have very different levels of SRP.

Linear modelling showed that GPP was best explained by both stream geomorphology and burn history at all except the smallest scales, where only geomorphology was a predictor; whereas respiration was best explained by stream geomorphology at almost all scales. P:R was best explained by watershed geomorphology at coarse scales and by burn history at finer scales. GPP's strong linkage with geomorphology at all scales but especially finer scales is likely due to the fact that local geomorphic setting dictates the long-term metabolic response to disturbance, and this is particularly true at reach scales. Because respiration is driven by a wider variety of variables than GPP in these systems (which is probably driven almost exclusively by light), it does not follow a similar pattern. The similar response by P:R is likely because P:R is driven by GPP in these systems.

We demonstrated that geomorphology has the strongest effect on GPP at the finest spatial resolutions, whereas burn history has the weakest effect at the finest scales. As you 'zoom

out' to coarser scales, the effect of burn history and geomorphology shift to have a nearly equal effect on GPP. It seems counterintuitive that geomorphology would have a stronger effect on GPP at a finer scale, but it is important to recognize that geomorphology incorporates stream width, which likely has the most effect at the finest scale. A similar pattern was observed for respiration. However, unlike GPP, the direction of the effect of burn history on respiration changed from fine to coarse resolutions: at fine resolutions more burn resulted in more respiration, while at coarse scales more burn did not result in more respiration. This may be because these ecological phenomena operate at different scales, or perhaps because the analysis is vulnerable to non-linearity or hysteresis when data from independent variables are at different resolutions.

Because the physical template is a filter for aquatic response to disturbance, there can be no overarching model of how all aquatic ecosystems will respond to wildfire. Local geomorphology, as well as specific limiting factors, geology, climate, and vegetation will all mediate stream succession after wildfire, in part because stream succession is so closely linked to terrestrial succession. Given this sensitivity to context, as well as dependence on the severity and frequency of disturbance, the two-dimensional conceptual model of postfire response curves used by Gresswell and others—with one axis for time and one axis for response—is inadequate to model the range of potential response scenarios. Instead, we suggest something more akin to a series of three-dimensional response "surfaces," with axes for time and response as well as geomorphic setting/climatic setting. For example, a series of response surfaces could be produced by looking at how ecosystems respond to fire along three axes (time, geomorphology and response) given a gradient of burn severity or frequency, with a different response surface for each point on the burn severity continuum. A similar series of three-axis response surfaces

could be created to visualize ecosystem response along a continuum of spatial scales, with each surface representing a given spatial scale.

Future research on stream ecosystem responses to fire should move in the direction of Verkaik et al. (2013) by focusing on how context (such as ecosystem type) impacts disturbance effects. By better understanding how specific stream types respond to disturbance, we can better react to and manage wildfire as climate change shifts fire regimes. Our study provides an important direction for understanding post-fire response of stream productivity across river networks.

Figures

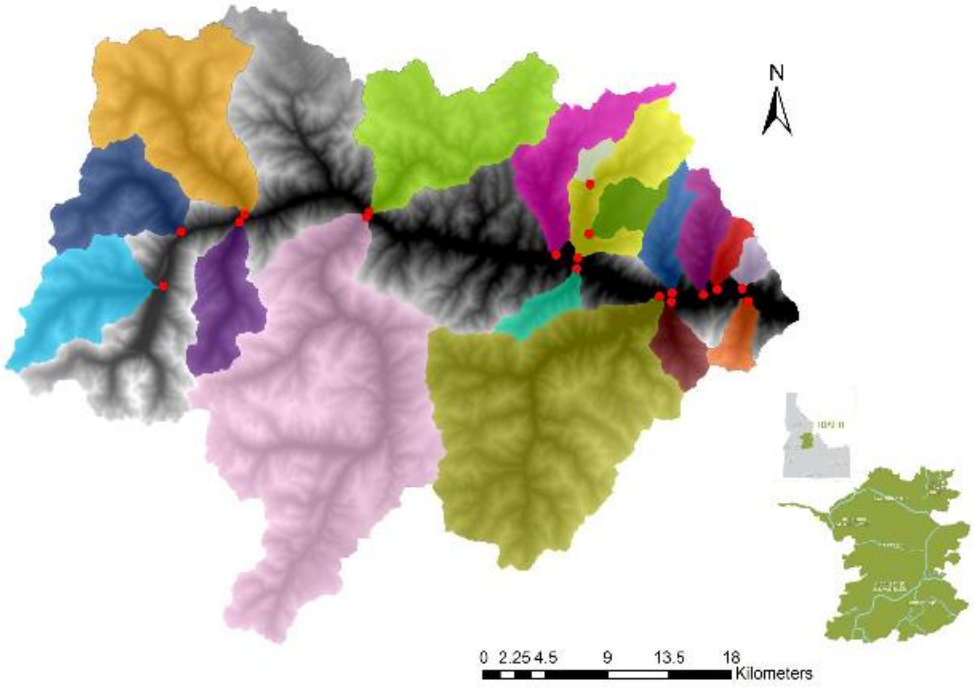

Figure 1. Big Creek watershed, overlain by 18 subwatersheds of interest; study sites are marked by red points. Inset shows Big Creek's location in central Idaho, USA.

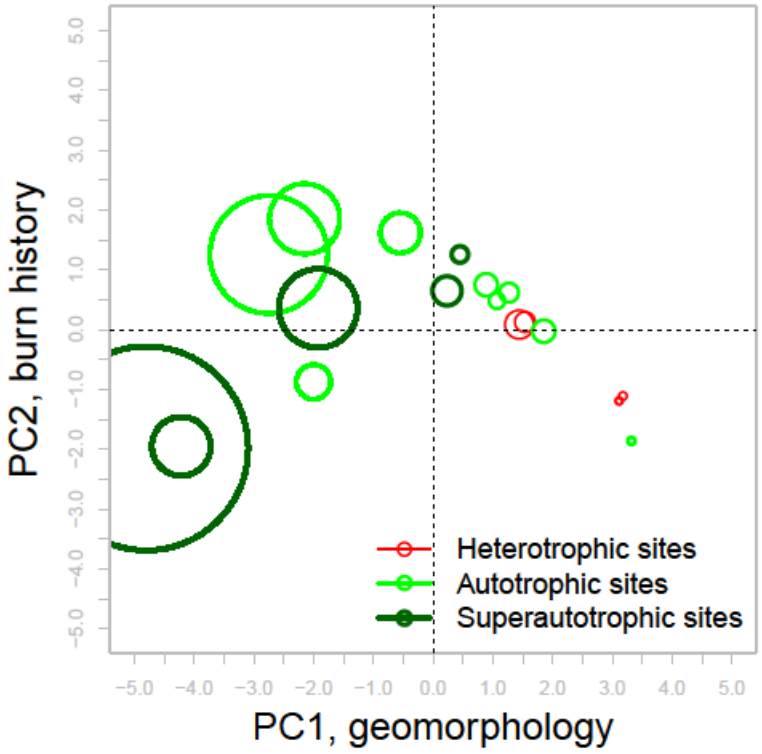

Figure 2. Principal component analysis for environmental data (stream geomorphology and burn history), watershed-scale.

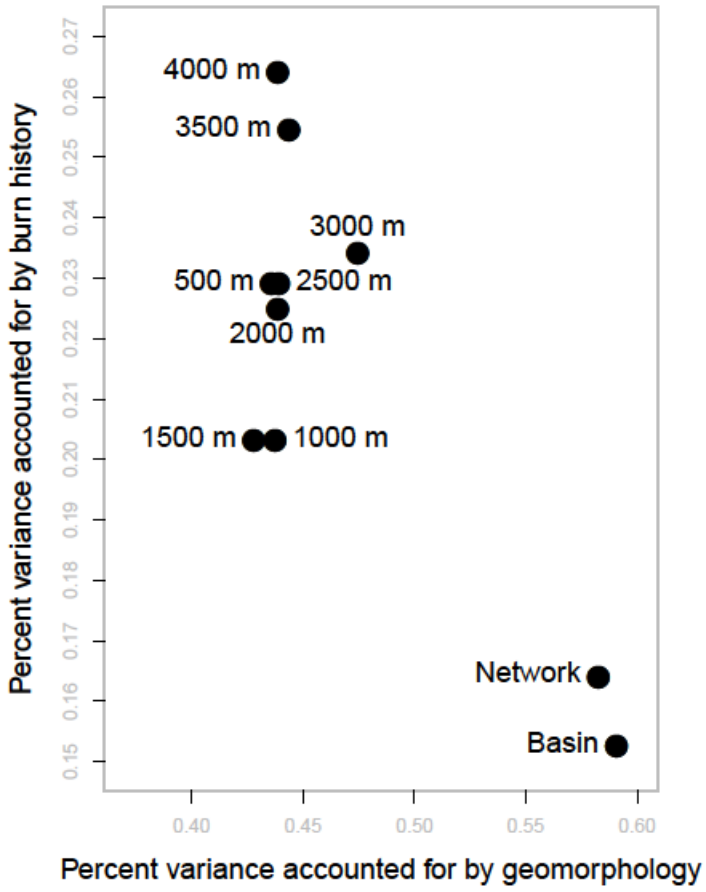

Figure 3. Percent variance explained by stream geomorphology versus burn history at each of ten scales of analysis.

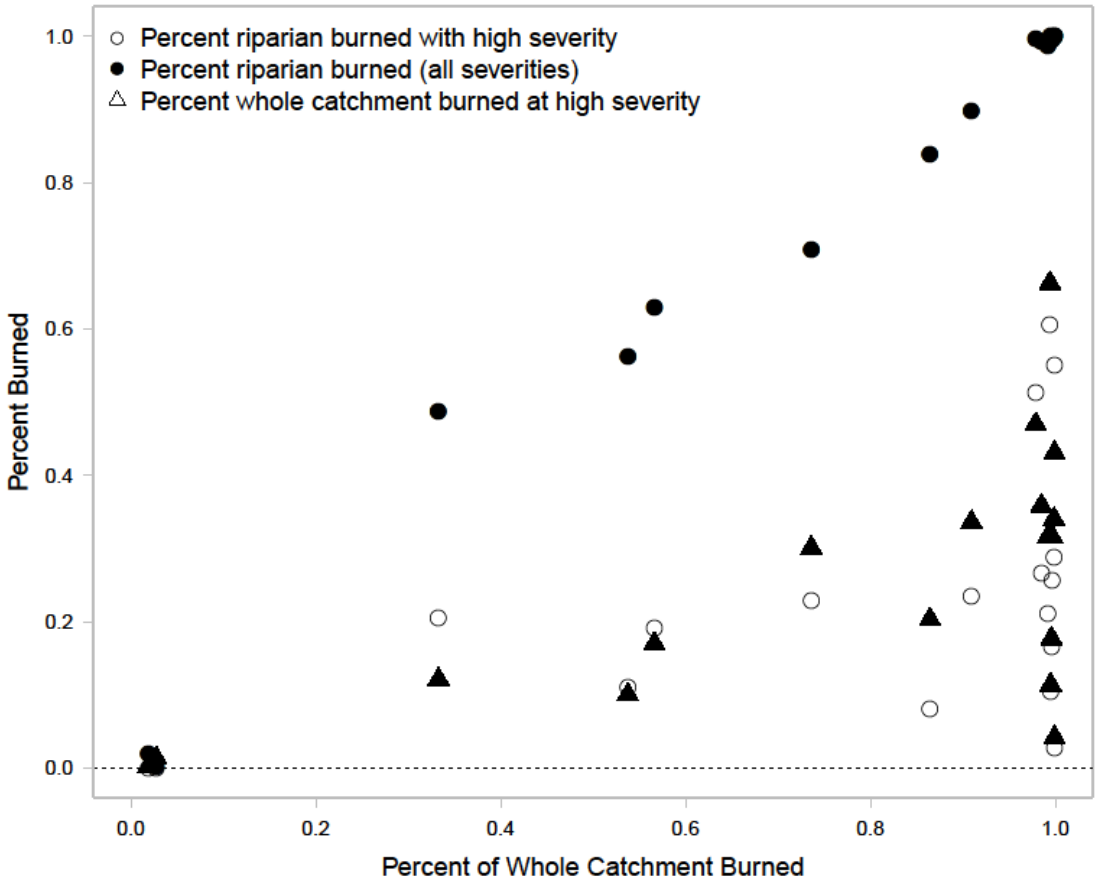

Figure 4. Percent of the entire watershed burned almost perfectly predicts total percent riparian burned over the entire area of a given stream network's riparian buffer. Percent watershed burned also predicts the percent of the network's riparian buffer burned.

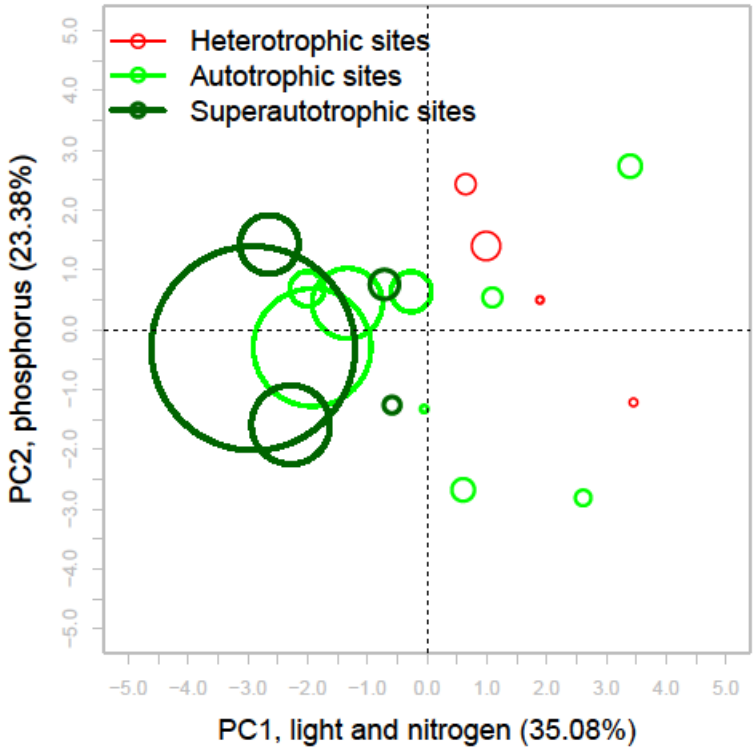

Figure 5. Principal component analysis of response variables (stream chemistry and light) from streams included in this study. ‘PC’= principal component; value in parentheses indicates the percentage of variance explained by each axis. 'TN.TP'=ratio of total nitrogen to total phosphorus; ‘DOC’=dissolved organic carbon; ‘TN’=total nitrogen; ‘TP’=total phosphorus. Open circles, which represent stream sites, are scaled by the mean width of the stream.

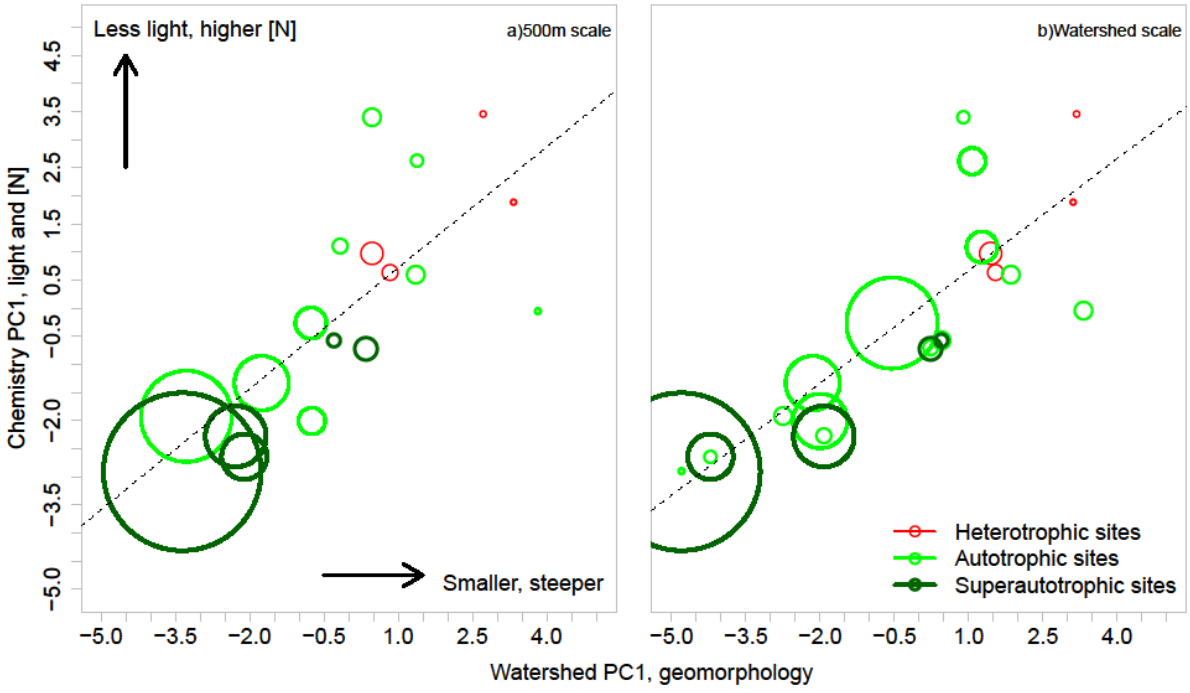

Figure 6a-b. Principal component regressions of response principal component 1 (light and nitrogen concentration) against explanatory principal component 1 (stream geomorphology) for the coarsest (watershed scale) and finest (500-m riparian buffer) spatial resolution in this study. 'PC'= principal component. Open circles, which represent streams, are scaled by the mean width of the stream.

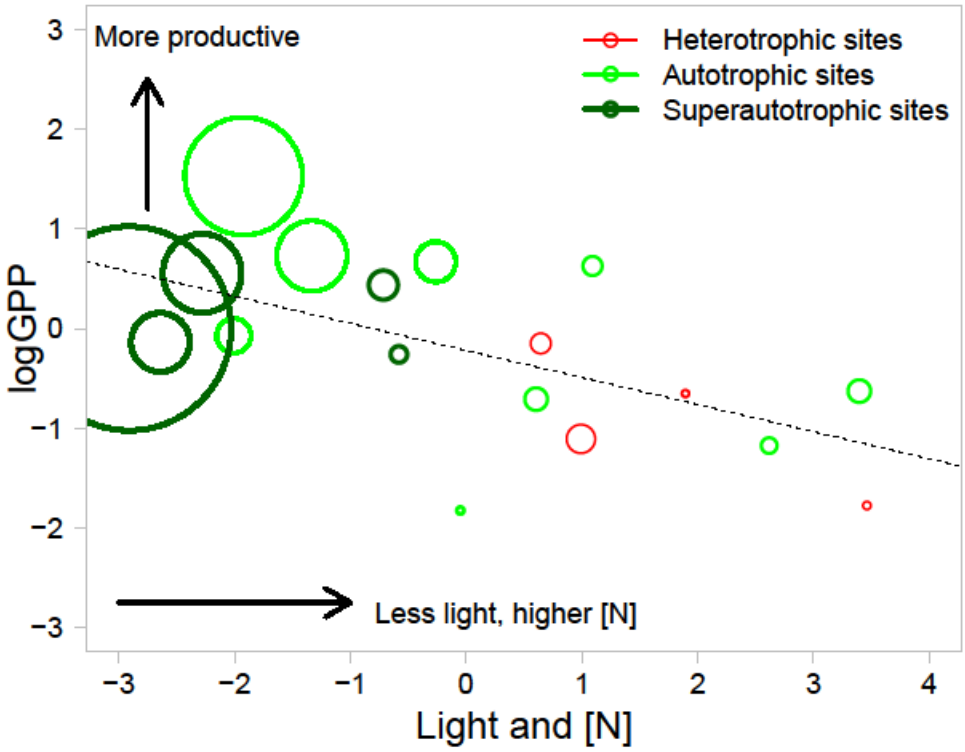

Figure 7. Principal component regression of response principal component 1 (light and nitrogen concentration) against the logged values of estimated gross primary productivity (GPP) for each study stream. 'PC'= principal component. Open circles, which represent streams, are scaled by the mean width of the stream.

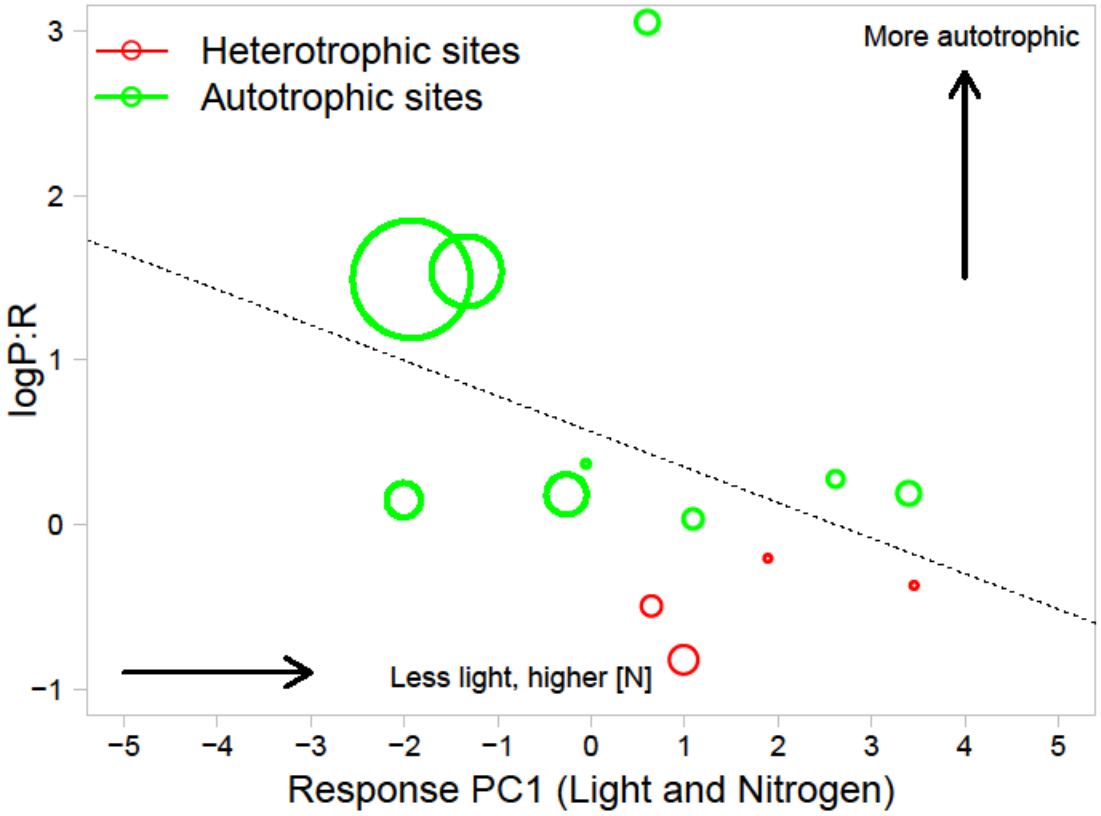

Figure 8. Principal component regression of response principal component 1 (light and nitrogen concentration) against the logged values of estimated whole-stream metabolism (P:R) for each stream for which a respiration value could be estimated. 'PC'= principal component. Open circles, which represent streams, are scaled by the mean width of the stream.

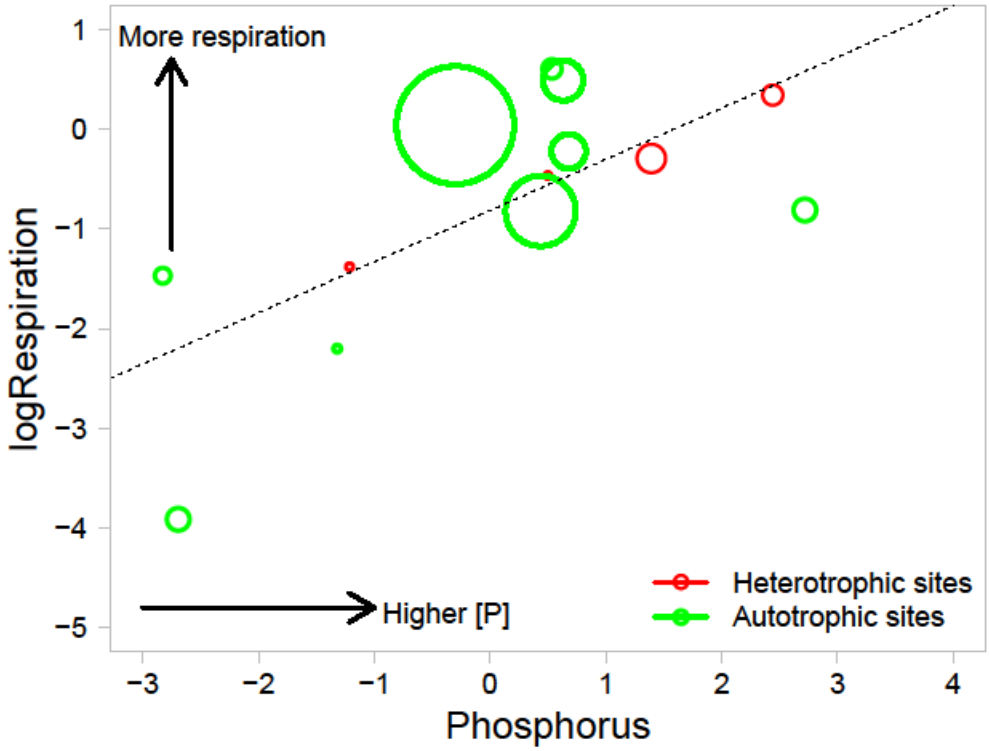

Figure 9. Principal component regression of response principal component 2 (phosphorus concentration) against the logged values of total respiration (Rt) for each stream for which a respiration value could be estimated. 'PC'= principal component. Open circles, which represent streams, are scaled by the mean width of the stream.

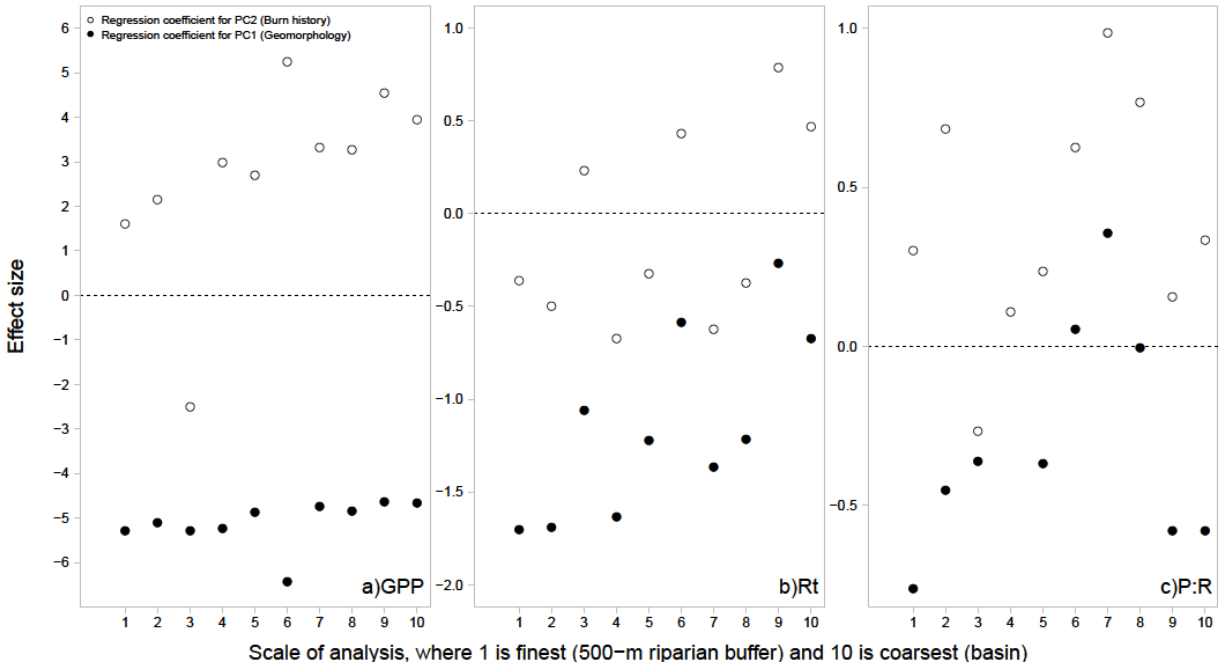

Figure 10 a-c. Effect size of environmental principal component 1 (stream geomorphology) and principal component 2 (burn history) plotted against scale of analysis (1=500-m riparian buffer, 2= 1000-m riparian buffer, and so on up to 9=network-scale riparian buffer, 10=watershed scale), from regressions against each of three response variables: a) gross primary productivity (GPP); b) total respiration (Rt); and c) whole-stream metabolism (P:R).

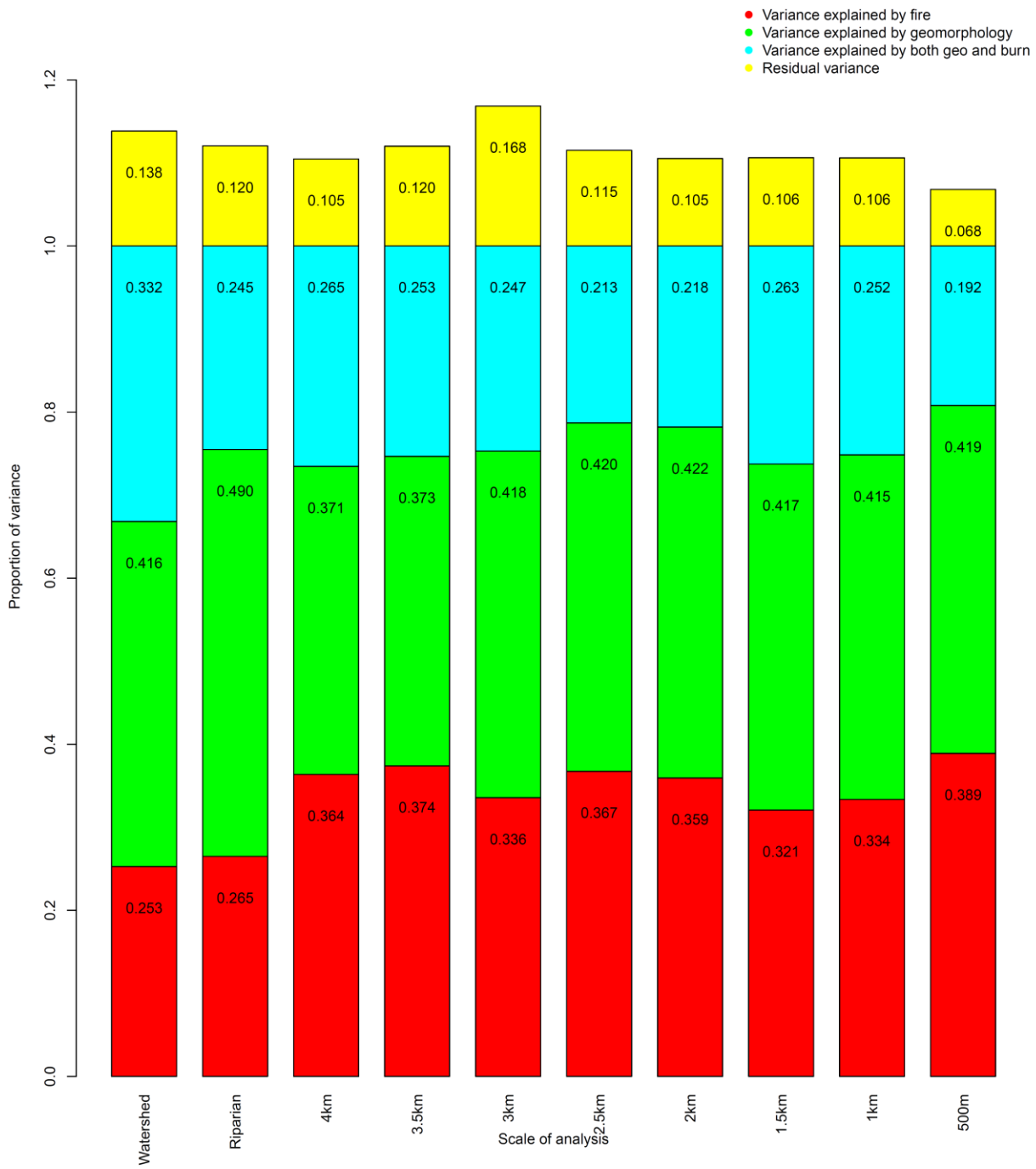

Figure 11. Results of partial redundancy analysis (pRDA): Marginal effects (variance attributable to single explanatory data sets without partialling out joint or confounding variation) of stream geomorphology vs. burn history on the response matrix, at each of ten spatial scales

Tables

Table 1. Results from response variables Principal Components Analysis (PCA) and explanatory variables PCA. The response variables PCA is based on stream chemical and light data collected from the 18 streams at the time of this study, while the explanatory variables PCA is based on fire history and geomorphic/physical data from the 18 streams. N:P = nitrogen: phosphorus ratio, DOC = dissolved organic carbon, TN = total nitrogen concentration, TP= total phosphorus concentration, TotalQ= stream discharge, AvgDepth= average depth, AvgWidth= average width, Low= percent burned with low severity, Area= watershed area, Slope= mean slope, PercentBurned= percent total watershed burned, Mod= percent burned with moderate severity, Severe= percent burned with high severity, VeryLow= percent burned with very low severity. *= significant axis based on 1000 random permutations.

Scale of analysis	Principal Component	Percent Variance Explained	Significance	Strong Variable Loadings (Structure correlations >= 0.4)
Basin	**Response Variables**			
	PC1	0.35	p<0.005*	ShadingRatio (-0.70), DOC (0.74), TN (0.84), NO_3^-(0.89), NO_2^-(0.76), TN:TP (0.46), SiO_4^{2-} (0.40)
	PC2	0.23	p<0.005*	TP (-0.59), PO_4^{3-} (-0.69), NH_4^+(0.82), TN:TP (0.70), SiO_4^{2-}(-0.65)
	Explanatory Variables			
	PC1	0.61	p<0.005*	AvgDepth (-0.86),- Area (-.77), MeanSlope (0.51), AvgWidth (-.93), TotalQ (-.90), PercentBurned (-.91), PercentVeryLow (0.68),PercentLow (0.83), PercentMod (0.79), PercentSevere (0.45)
	PC2	0.15	p=0.99	AvgDepth (0.43),Area (0.50),PercentMod (0.49),PercentSevere (0.71)
Network-scale riparian	**Explanatory Variables**			
	PC1	0.58	p<0.005*	AvgDepth (-0.84),- Area (-.66), MeanSlope (0.80), AvgWidth (-.93), TotalQ (-.90), PercentBurned (-.93), PercentLow (0.77), PercentMod (0.78), PercentSevere (0.46)
	PC2	0.16	p=0.93	
4 km riparian	**Explanatory Variables**			
	PC1	0.44	p<0.005*	AvgDepth (-0.89), AvgWidth (-0.94), TotalQ (-0.93), Low (0.43), Area (-0.82), Slope (0.86)
	PC2	0.26	p<0.005*	PercentBurned (0.90), Very Low (0.59), Low (0.78), Mod (0.69), Area (0.50)
	PC3	0.18	p=0.01*	Very Low (0.66), Mod (-0.57), Severe (-0.85)
3.5 km riparian	**Explanatory Variables**			
	PC1	0.44	p<0.005*	AvgDepth (-0.89), AvgWidth (-0.94), TotalQ (-0.92), Low (0.51), Area (-0.81), Slope (0.84)

	PC2	0.25	p<0.005*	PercentBurned (0.90), VeryLow (0.5), Low (0.71), Mod (0.72), Area (0.51)
	PC3	0.19	p<0.005*	Very Low (0.74), Low (0.41), Mod (-0.53), Severe (-0.85)
3 km riparian	**Explanatory Variables**			
	PC1	0.47	p<0.005*	AvgDepth (-0.88), AvgWidth (-0.94),TotalQ (-0.90), PercentBurned (0.48), Very Low (0.49), Low (0.66), Area (-0.83), Slope (0.81)
	PC2	0.23	p=0.01*	PercentBurned (0.82), Mod (0.91), Severe (0.58), Area (0.47)
	PC3	0.19	p=0.01*	VeryLow (0.780), Low (0.61), Severe (-0.68)
2.5 km riparian	**Explanatory Variables**			
	PC1	0.44	p<0.005*	AvgDepth (-0.90), AvgWidth (-0.95), TotalQ (-0.95), Area (0.85), Slope (0.84)
	PC2	0.23	p=0.02*	PercentBurned (0.90), Very Low (0.60), Low (0.79), Mod (0.47), Area (0.43)
	PC3	0.21	p<0.005*	Very Low (-0.68), Mod (0.79), Severe (0.85)
2 km riparian	**Explanatory Variables**			
	PC1	0.44	p<0.005*	AvgDepth (-0.90), AvgWidth (-0.95), Total Q (-0.95), Low (0.45), Area (-0.86), Slope (0.8)
	PC2	0.23	p=0.01*	PercentBurned (0.87), Mod (0.90), Severe (0.54), Area (0.41)
	PC3	0.20	p<0.005*	Very Low (0.85), Low (0.72), Severe (-0.68)
1.5 km riparian	**Explanatory Variables**			
	PC1	0.43	p<0.005*	AvgDepth (-0.91),AvgWidth (-0.95), TotalQ (-0.96), Area (-0.88), Slope (0.77)
	PC2	0.20	p=0.18	PercentBurned (-0.96), Low (-0.66), Moderate (-0.65)
	PC3	0.19	p=0.005*	VeryLow (0.75),Low (0.49),Mod (-0.69), Severe (-0.76)
1 km riparian	**Explanatory Variables**			
	PC1	0.44	p<0.005*	AvgDepth (-0.91),AvgWidth (-0.95),TotalQ (-0.95),Low (0.51), Area (-0.88),Slope (0.79)
	PC2	0.20	p=0.19	PercentBurned (.91), Low (0.50), Mod (0.84)
	PC3	0.14	p=0.772	Very Low (-0.83), Low (-0.463), Mod (0.47)
500 m riparian	**Explanatory Variables**			
	PC1	0.46	p<0.005*	AvgDepth (-0.92),AvgWidth (-0.95),TotalQ (-0.93),Low (0.57),Area (-0.87), Slope (0.76)
	PC2	0.23	p=0.01*	PercentBurned (0.92),Low (0.57), Mod (0.78),Severe (0.62)
	PC3	0.16	p=0.21	VeryLow (-0.91),Low (-0.44), Mod (0.50), Severe (0.46)

Table 2a. Percent total watershed burned predicts total percent burned at other scales.

Scale of analysis	r	F	df	p
500-m riparian	0.84	89.92	17	<0.01
1 km riparian	0.90	147.40	17	<0.01
1.5 km riparian	0.91	166.80	17	<0.01
2 km riparian	0.91	175.50	17	<0.01
2.5 km riparian	0.91	177.60	17	<0.01
3 km riparian	0.92	189.10	17	<0.01
3.5 km riparian	0.92	182.90	17	<0.01
4 km riparian	0.91	168.70	17	<0.01
Network-scale riparian	1.00	7145	17	<0.01

Table 2b. Percent total watershed burned predicts percent burned with high severity at some other scales.

Scale of analysis	r	F	df	p
500-m riparian	0.15	3.03	17	0.10
1 km riparian	0.10	1.85	17	0.19
1.5 km riparian	0.17	3.43	17	0.08
2 km riparian	0.29	6.99	17	0.02
2.5 km riparian	0.30	7.39	17	0.01
3 km riparian	0.29	7.00	17	0.02
3.5 km riparian	0.34	8.66	17	<0.01
4 km riparian	0.28	6.58	17	0.02
Network-scale riparian	0.73	45.56	17	<0.01
Watershed	0.81	71.23	17	<0.01

Table 3. Ranges of physical, geomorphic, and chemical characteristics of streams sampled in this study. TN = Total nitrogen; TP= Total phosphorus; N:P= Nitrogen to phosphorus ratio; DOC= Dissolved organic carbon; *Chl-a* = Chlorophyll-a.

Variable	**Range**
TN (μg L^{-1})	79.40-457.89
TP (μg L^{-1})	9.50-30.80
N:P	4.80-34.43
PO_4^{3-} (μg L^{-1})	0.30-4.50
NO_3^- (μg L^{-1})	0.00-407.5
NO_2^- (μg L^{-1})	0.3-2.00
NH_4^+ (μg L^{-1})	0.00-3.2
DOC (mg L^{-1})	2.32-6.62
SiO_4^{4-} (μg L^{-1})	3925.6-7655.30
Chl-a (μg cm^{-2})	1.26-20.69
Shading Ratio	0.10-1.58
Total % Watershed Burned	2-100
Total % Riparian Zone Burned	0-100
% Very Low Severity	0-45
% Low Severity	0-38
% Moderate Severity	0-41
% Severe	0-66
Average Width (m)	0.88-23.58
Average Depth (m)	0.04-0.36
Average Watershed Slope (degrees)	21.72-32.51
Watershed Area (km^2)	4993000-325506900
Stream Discharge (cms^{-1})	0.01-1.10

Table 4. Principal Component Regressions. *= significant ($p \leq 0.05$), **= marginally significant ($0.25 \geq p > 0.05$). Response PC1 captures variation among streams in total nitrogen concentration and light, while Response PC2 captures variation in phosphorus concentration. PC1 and PC2 refer to the scale-specific principal components of the explanatory variables PCA; for each scale, PC1 captures variation in that scale's geomorphic characteristics, while PC2 captures the variation in burn history. GPP= gross primary production, Rt= total respiration, PR= ratio of gross primary production to total respiration.

Scale of analysis	Model	β0 (SE)	β1 (SE)	p-value β0	p-value β1	R^2	F	df	Overall p-value
500-m riparian	ResponsePC1~ β1PC1		0.72 (0.15)		<<0.005	0.56	21.71	17	<<0.005
1000-m riparian	ResponsePC1~ β1PC1		0.75 (0.14)		<<0.005	0.61	27.05	17	<<0.005
1500-m riparian	ResponsePC1~ β1PC1		0.77 (0.14)		<<0.005	0.64	29.85	17	<<0.005
2000-m riparian	ResponsePC1~ β1PC1		0.76 (0.14)		<<0.005	0.64	29.74	17	<<0.005
2500-m riparian	ResponsePC1~ β1PC1		0.77 (0.14)		<<0.005	0.65	31.63	17	<<0.005
3000-m riparian	ResponsePC1~ β1PC1		0.72 (0.14)		<<0.005	0.62	27.22	17	<<0.005
3500-m riparian	ResponsePC1~ β1PC1		0.76 (0.14)		<<0.005	0.65	31.42	17	<<0.005
4000-m riparian	ResponsePC1~ β1PC1		0.78 (0.13)		<<0.005	0.67	34.36	17	<<0.005
Network riparian	ResponsePC1~ β1PC1		0.68 (0.11)		<<0.005	0.68	35.71	17	<<0.005
Basin	ResponsePC1~ β1PC1		0.67 (0.11)		<<0.005	0.67	35.09	17	<<0.005
Other	GPP~ β1ResponsePC1		-0.27 (0.09)		0.009*	0.34	8.73	17	0.009
	PR~ β0+ β1ResponsePC1	0.56 (0.30)	-0.22 (0.16)	0.09*	0.2**	0.14	1.84	17	0.20
	Rt~ β0+ β1ResponsePC2	-0.82 (0.26)	0.51 (0.16)	0.009*	0.007*	0.49	10.81	17	0.007
	PR~ β0+ β1ResponsePC2	0.44 (0.26)	-0.31 (0.16)	0.12**	0.075**	0.26	3.85	17	0.075

Table 5. Metabolism parameters for each of 18 study streams. Respiration models: 1= No biological activity ([O2] governed only by physical parameters) ; 2= Temperature-sensitive CR using only one carbon substrate (Rb), using Equation 3; 3= Temperature- sensitive CR using only one carbon substrate and equation 6; 4= Constant CR, where CR is assumed not to respond to temperature; 5= Temperature-sensitive CR using two carbon sources (Rb and Rp) using photosynthesis from the previous timestep (Equation 4); 6= Temperature-sensitive CR using two carbon sources (Rb and Rp), calculated with a weighted average of the previous 30 minutes of estimated photosynthesis (Equation 5)

Stream	GPP (g O_2 m^{-2} d^{-1})	Rb (g O_2 m^{-2} d^{-1})	Rp (g O_2 m^{-2} d_{-1})	Rt (g O^2 m_{-2} d^{-1})	Rp:Rb	P:R	G (g O_2 m^{-2} d^{-1})	K_{20} (m h^{-1})	α	α-PI	P_{max} (mg m^{-2} h^{-1})	O_2start (mg m^{-3})	σ (mg m^{-3})	Best respiration model
Beaver	2.07	0.44	n/a	0.44	n/a	4.66	-1.61	2.85	n/a	5.96	258.48	9162.63	18.56	3
Burnt	0.33	0.44	0.32	0.75	0.72	0.44	0.42	0.36	1.43	5.62	76.11	9387.58	27.73	6
Cabin	0.77	0.00	0.00	0.00	0.00	n/a	-0.76	0.43	n/a	1.88	168.87	8339.8	48.29	no model could be determined
Canyon	0.49	0.02	n/a	0.02	n/a	21.03	-0.47	0.2192	n/a	2.78	227.53	9386.66	34.29	3
Cave	1.57	0.00	0.00	0.00	0.00	n/a	-1.56	0.62	n/a	4.8	425.57	9173.03	44.32	no model could be determined
Cliff	0.53	0.00	0.44	0.44	>>>10e^3	1.20	-0.08	0.38	1.17	2.92	142.76	9055.08	14.40	6
Cougar	1.86	0.05	1.76	1.81	38.19	1.03	-0.04	0.15	1.23	21.99	398.63	9262.29	33.15	5
Cow	0.31	0.00	0.23	0.23	>>>10e^3	1.32	-0.07	0.23	1.11	2.38	155.53	9626.88	31.27	6
Crooked	1.95	0.00	1.63	1.63	>>>10e^3	1.20	-0.38	0.27	1.12	10.95	395.13	8298.95	51.17	6
Dunce	0.52	0.13	0.50	0.63	3.74	0.81	0.11	0.22	1.26	9.84	225.46	8971.16	19.75	6
Goat	0.17	0.09	0.17	0.25	1.97	0.69	0.07	0.11	1.36	2.74	117.02	9169.16	21.04	6
Logan	1.00	0.00	0.00	0.00	0.00	n/a	-0.98	1.22	n/a	3.13	223.69	9074.89	14.39	no model could be determined
Marble	0.93	0.00	0.80	0.80	>>>10e^3	1.16	-0.10	0.77	1.43	18.96	182.32	9670.18	12.81	5
Monumental	4.61	0.32	0.94	1.04	2.90	4.44	-0.42	0.67	0.82	2.08	707.06	8607.11	57.34	6
Northfork	0.16	0.02	0.10	0.11	5.82	1.45	-0.05	0.17	0.83	5.63	189.83	8802.66	23.63	6
Pioneer	0.86	0.61	0.81	1.42	1.33	0.61	0.55	0.63	1.42	13.00	247.38	9582.34	25.14	6
Rush	1.74	0.00	0.00	0.00	0.00	n/a	-1.74	0.34	n/a	7.85	338.03	9023.08	38.55	no model could be determined
Smith	0.87	0.00	0.00	0.00	0.00	n/a	-0.86	1.65	n/a	3.00	126.48	9182.80	16.06	no model could be determined

Table 6a. Range of models predicting the effect of burn history, watershed geomorphology, and their interaction on rates of gross primary productivity in streams in this study. Models were compared using AICc. βo = the estimated intercept, βn= the model- specific estimated slope of parameter *n*, N = sample size, k = number of parameters, SE= standard error. Δ AIC_c is the difference between each model-specific AIC_c value and the lowest AIC_c value within the set of models in a given scale; and AIC_c w_i is the model weight for each model considered. Highlighted models are the top models (Δ AIC_c = 0) for a given scale.

General model form for all models considered

GPP~ $\beta 0 + \beta 1PC1 + \beta 2PC2 + \ldots.\beta_n$

Scale of Analysis	Models Considered	β0 (SE)	β1 (SE)	β2 (SE)	β3 (SE)	R^2	N	k	AIC_c	Δ AIC_c	AIC_c w_i
Basin	GPP~ β0 + β1PC1 + β2PC2	-0.22 (0.12)	-0.24 (0.05)	0.40 (0.10)		0.71	18.00	4.00	35.07	0.00	0.82
	GPP~β0 + β1PC1 + β2PC2 + β3PC1*PC2	-0.22 (0.12)	-0.27 (0.08)	0.36 (0.13)	-0.04 (0.05)	0.73	18.00	5.00	38.17	3.10	0.17
Network-scale Riparian	GPP~ β0 + β1PC1 + β2PC2	-0.22 (0.12)	-0.23 (0.05)	0.42 (0.09)		0.74	18.00	4.00	33.42	0.00	0.87
	GPP~β0 + β1PC1 + β2PC2 + β3PC1*PC2	-0.22 (0.12)	-0.23 (0.08)	0.42 (0.13)	0.00 (0.05)	0.74	18.00	5.00	37.34	3.92	0.12
4 km	GPP~ β0 + β1PC1 + β2PC2	-0.22 (0.13)	-0.30 (0.06)	0.26 (0.08)		0.69	18.00	4.00	36.14	0.00	0.50
	GPP~β0 + β1PC1+ β2PC2 + β3PC3	-0.22 (0.12)	-0.30 (0.06)	0.26 (0.08)	-0.14 (0.09)	0.74	18.00	5.00	37.41	1.27	0.26
	GPP~β0 + β1PC1 + β2PC2 + β3PC1*PC2	-0.22 (0.13)	-0.36 (0.09)	0.12 (0.16)	-0.06 (0.07)	0.71	18.00	5.00	38.97	2.83	0.12
3.5 km	GPP~β0 + β1PC1+ β2PC2 + β3PC3	-0.22	-0.29	0.27	-0.20	0.78	18.00	5.00	33.92	0.00	0.60
	GPP~ β0 + β1PC1 + β2PC2	-0.22	-0.29	0.27		0.69	18.00	4.00	36.38	2.45	0.17
3 km	GPP~ β0 + β1PC1 + β2PC2	-0.22	-0.29	0.34		0.82	18.00	4.00	26.53	0.00	0.73
	GPP~β0 + β1PC1 + β2PC2 + β3PC1*PC2	-0.22	-0.27	0.36	0.01	0.82	18.00	5.00	30.25	3.72	0.11
	GPP~β0 + β1PC1+ β2PC2 + β3PC3	-0.22	-0.29	0.34	0.03	0.82	18.00	5.00	30.31	3.78	0.11
2.5 km	GPP~ β0 + β1PC1 + β2PC2	-0.22	-0.31	0.24		0.67	18.00	4.00	37.33	0.00	0.44
	GPP~β0 + β1PC1+ β2PC2 + β3PC3	-0.22	-0.31	0.24	0.13	0.72	18.00	5.00	38.75	1.42	0.22
	GPP~β0 + β1PC1 + β2PC2 + β3PC1*PC2	-0.22	-0.38	0.05	-0.09	0.71	18.00	5.00	39.31	1.98	0.16
	GPP~ β0 + β1PC1	-0.22	-0.31			0.52	18.00	3.00	41.05	3.72	0.07

2 km	GPP~ β0 + β1PC1 + β2PC2	-0.22	-0.32	0.25		0.71	18.00	4.00	35.32	0.00	0.63
	GPP~β0 + β1PC1+ β2PC2 + β3PC3	-0.22	-0.32	0.25	0.06	0.72	18.00	5.00	38.60	3.28	0.12
	GPP~β0 + β1PC1 + β2PC2 + β3PC1*PC2	-0.22	-0.32	0.23	-0.01	0.71	18.00	5.00	39.19	3.87	0.09
1.5 km	GPP~ β0 + β1PC1 + β2PC2	-0.22	-0.33	-0.23		0.70	18.00	4.00	36.11	0.00	0.57
	GPP~ β0 + β1PC1	-0.22	-0.33			0.57	18.00	3.00	39.08	2.97	0.13
	GPP~β0 + β1PC1+ β2PC2 + β3PC3	-0.22	-0.33	-0.23	-0.08	0.71	18.00	5.00	39.21	3.10	0.12
	GPP~β0 + β1PC1 + β2PC2 + β3PC1*PC2	-0.22	-0.35	-0.12	0.05	0.70	18.00	5.00	39.69	3.58	0.10
1 km	GPP~ β0 + β1PC1 + β2PC2	-0.22	-0.33	0.20		0.67	18.00	4.00	37.39	0.00	0.46
	GPP~ β0 + β1PC1	-0.22	-0.33			0.57	18.00	3.00	38.93	1.54	0.21
	GPP~β0 + β1PC1 + β2PC3 + β3PC1*PC3	-0.22	-0.38	-0.04	0.15	0.68	18.00	5.00	40.63	3.24	0.09
	GPP~β0 + β1PC1 + β2PC2 + β3PC1*PC2	-0.22	-0.34	0.13	-0.04	0.68	18.00	5.00	40.71	3.32	0.09
	GPP~β0 + β1PC1+ β2PC2 + β3PC3	-0.22	-0.33	0.20	-0.05	0.68	18.00	5.00	41.11	3.72	0.07
500 m	GPP~ β0 + β1PC1	-0.22	-0.34			0.61	18.00	3.00	37.04	0.00	0.38
	GPP~ β0 + β1PC1 + β2PC2	-0.22	-0.34	0.14		0.67	18.00	4.00	37.51	0.46	0.30
	GPP~β0 + β1PC1 + β2PC2 + β3PC1*PC2	-0.22	-0.37	0.01	-0.08	0.71	18.00	5.00	39.22	2.18	0.13
	GPP~ β0 + β1PC1 + β2PC3	-0.22	-0.34	0.01		0.61	18.00	4.00	40.40	3.36	0.07

Table 6b. Range of models predicting the effect of burn history (PC2, PC3), watershed geomorphology (PC1), and their interaction on rates of total respiration in streams in this study. Models were compared using AIC_c. β_o = the estimated intercept, β_n= the model-specific estimated slope of parameter *n*, N = sample size, k = number of parameters, SE= standard error. Δ AIC_c is the difference between each model-specific AIC_c value and the lowest AIC_c value within the set of models in a given scale; and AIC_c w_i is the model weight for each model considered. Highlighted models are the top models (Δ AIC_c = 0) for a given scale.

General model form for all models considered Rt~ β0 + β1PC1 + β2PC2 + ….β_n										
Scale of analysis	**Models Considered**	**β0 (SE)**	**β1 (SE)**	**β2 (SE)**	**R^2**	**N**	**k**	**AIC_c**	**Δ AIC_c**	**AIC_c w_i**
Basin	Rt~ β0 + β1PC1	-0.59	-0.24		0.15	13.00	3.00	48.20	0.00	0.50
	Rt~ β0 + β1PC2	-0.83	0.40		0.13	13.00	3.00	48.49	0.29	0.43
Network-scale Riparian	Rt~ β0 + β1PC2	-0.81	0.52		0.20	13.00	3.00	47.51	0.00	0.54
	Rt~ β0 + β1PC1	-0.57	-0.26		0.15	13.00	3.00	48.20	0.69	0.39
4 km riparian	Rt~ β0 + β1PC1	-0.57	-0.30		0.19	13.00	3.00	47.62	0.00	0.48
	Rt~ β0 + β1PC2	-0.83	0.30		0.08	13.00	3.00	49.23	1.61	0.21
	Rt~ β0 + β1PC3	-0.81	-0.14		0.03	13.00	3.00	50.01	2.39	0.14
3.5 km riparian	Rt~ β0 + β1PC1	-0.55	-0.31		0.20	13.00	3.00	47.38	0.00	0.45
	Rt~ β0 + β1PC2	-0.84	0.33		0.09	13.00	3.00	49.11	1.73	0.19
	Rt~ β0 + β1PC3	-0.83	-0.24		0.07	13.00	3.00	49.34	1.96	0.17
	Rt~ β0 + β1PC1 + β2PC3	-0.61	-0.29	-0.15	0.23	13.00	4.00	51.21	3.83	0.07
	Rt~ β0 + β1PC1 + β2PC2	-0.34	-0.52	-0.37	0.23	13.00	4.00	51.21	3.84	0.07
3 km riparian	Rt~ β0 + β1PC1	-0.55	-0.32		0.23	13.00	3.00	46.93	0.00	0.40
	Rt~ β0 + β1PC2	-0.91	0.51		0.22	13.00	3.00	47.13	0.19	0.36
	Rt~ β0 + β1PC3	-0.79	-0.08		0.01	13.00	3.00	50.23	3.30	0.08
2.5 km riparian	Rt~ β0 + β1PC1	-0.56	-0.31		0.21	13.00	3.00	47.27	0.00	0.50
	Rt~ β0 + β1PC2	-0.84	0.39		0.10	13.00	3.00	48.95	1.67	0.22
	Rt~ β0 + β1PC3	-0.79	0.05		0.00	13.00	3.00	50.30	3.03	0.11
2 km riparian	Rt~ β0 + β1PC1	-0.57	-0.30		0.21	13.00	3.00	47.29	0.00	0.52
	Rt~ β0 + β1PC2	-0.85	0.24		0.04	13.00	3.00	49.79	2.50	0.15
	Rt~ β0 + β1PC3	-0.77	0.17		0.04	13.00	3.00	49.84	2.55	0.14
	Rt~ β0 + β1PC1 + β2PC2	-0.39	-0.43	-0.32	0.24	13.00	4.00	51.04	3.76	0.08
1.5 km riparian	Rt~ β0 + β1PC1	-0.58	-0.29		0.20	13.00	3.00	47.52	0.00	0.45
	Rt~ β0 + β1PC2	-0.88	-0.51		0.11	13.00	3.00	48.82	1.31	0.23
	Rt~ β0 + β1PC3	-0.75	0.14		0.03	13.00	3.00	49.95	2.43	0.13

	Rt~ β0 + β1PC1 + β2PC3	-0.55	-0.30	0.16	0.24	13.00	4.00	51.16	3.64	0.07
1 km riparian	Rt~ β0 + β1PC1	-0.58	-0.30		0.22	13.00	3.00	47.16	0.00	0.57
	Rt~ β0 + β1PC2	-0.81	0.16		0.02	13.00	3.00	50.10	2.94	0.13
	Rt~ β0 + β1PC3	-0.78	-0.01		0.00	13.00	3.00	50.35	3.19	0.12
500 km riparian	Rt~ β0 + β1PC1	-0.60	-0.30		0.23	13.00	3.00	47.03	0.00	0.59
	Rt~ β0 + β1PC2	-0.81	0.11		0.01	13.00	3.00	50.17	3.14	0.12
	Rt~ β0 + β1PC3	-0.78	0.05		0.00	13.00	3.00	50.30	3.28	0.11

Table 6c. Range of models predicting the effect of burn history (PC2, PC3), watershed geomorphology (PC1), and their interaction on rates of whole-stream metabolism (P:R) in streams in this study. Models were compared using AIC_c. β_o = the estimated intercept, β_n= the model-specific estimated slope of parameter *n*, N = sample size, k = number of parameters, SE= standard error. Δ AIC_c is the difference between each model-specific AIC_c value and the lowest AIC_c value within the set of models in a given scale; and AIC_c w_i is the model weight for each model considered. Highlighted models are the top models (Δ AIC_c = 0) for a given scale.

General model form for all models considered

P:R~ $\beta 0 + \beta 1PC1 + \beta 2PC2 + ...\beta_n$

Scale of Analysis	Models Considered	β0 (SE)	β1 (SE)	β2 (SE)	R^2	N	k	AIC_c	Δ AIC_c	$AICc$ w_i
Basin	PR~ β0 + β1PC1	0.54	-0.17		0.11	13.00	3.00	44.13	0.00	0.50
	PR~ β0 + β1PC2	0.38	0.27		0.09	13.00	3.00	44.42	0.28	0.43
Network-scale Riparian	PR~ β0 + β1PC1	0.56	-0.18		0.11	13.00	3.00	44.12	0.00	0.51
	PR~ β0 + β1PC2	0.40	0.28		0.08	13.00	3.00	44.52	0.40	0.42
4km	PR~ β0 + β1PC2	0.36	0.33		0.14	13.00	3.00	43.59	0.00	0.41
	PR~ β0 + β1PC1	0.54	-0.18		0.09	13.00	3.00	44.34	0.75	0.28
	PR~ β0 + β1PC3	0.40	-0.04		0.00	13.00	3.00	45.58	1.99	0.15
3.5 km	PR~ β0 + β1PC2	0.35	0.35		0.15	13.00	3.00	43.49	0.00	0.44
	PR~ β0 + β1PC1	0.53	-0.16		0.08	13.00	3.00	44.53	1.05	0.26
	PR~ β0 + β1PC3	0.41	-0.02		0.00	13.00	3.00	45.61	2.12	0.15
3 km	PR~ β0 + β1PC2	0.34	0.29		0.10	13.00	3.00	44.21	0.00	0.35
	PR~ β0 + β1PC1	0.52	-0.14		0.07	13.00	3.00	44.70	0.49	0.28
	PR~ β0 + β1PC3	0.43	0.11		0.02	13.00	3.00	45.33	1.13	0.20
	PR~ β0 + β1PC2 + β2PC3	0.34	0.34	0.17	0.16	13.00	4.00	47.76	3.55	0.06
2.5 km	PR~ β0 + β1PC1	0.53	-0.16		0.08	13.00	3.00	44.47	0.00	0.31
	PR~ β0 + β1PC2	0.37	0.28		0.08	13.00	3.00	44.58	0.10	0.30
	PR~ β0 + β1PC3	0.38	0.14		0.04	13.00	3.00	45.12	0.65	0.23
	PR~ β0 + β1PC2 + β2PC3	0.29	0.37	0.22	0.16	13.00	4.00	47.66	3.18	0.06
2 km	PR~ β0 + β1PC2	0.29	0.44		0.20	13.00	3.00	42.78	0.00	0.49
	PR~ β0 + β1PC1	0.53	-0.17		0.09	13.00	3.00	44.40	1.62	0.22
	PR~ β0 + β1PC3	0.41	-0.09		0.02	13.00	3.00	45.42	2.63	0.13
1.5 km	PR~ β0 + β1PC3	0.37	-0.25		0.13	13.00	3.00	43.73	0.00	0.32
	PR~ β0 + β1PC1	0.53	-0.17		0.10	13.00	3.00	44.24	0.51	0.24

	PR~ β0 + β1PC2	0.33	-0.39		0.09	13.00	3.00	44.32	0.59	0.23
	PR~ β0 + β1PC2 + β2PC3	0.29	-0.38	-0.24	0.23	13.00	4.00	46.63	2.90	0.07
	PR~ β0 + β1PC1 + β2PC3	0.48	-0.16	-0.23	0.22	13.00	4.00	46.71	2.98	0.07
1 km	PR~ β0 + β1PC2	0.35	0.32		0.11	13.00	3.00	44.14	0.00	0.36
	PR~ β0 + β1PC1	0.51	-0.16		0.08	13.00	3.00	44.47	0.33	0.31
	PR~ β0 + β1PC3	0.41	-0.01		0.00	13.00	3.00	45.61	1.48	0.17
	PR~ β0 + β1PC2 + β2PC3	0.32	0.41	-0.16	0.14	13.00	4.00	48.00	3.86	0.05
500 m	PR~ β0 + β1PC1	0.50	-0.16		0.09	13.00	3.00	44.40	0.00	0.38
	PR~ β0 + β1PC2	0.37	0.17		0.04	13.00	3.00	45.02	0.62	0.28
	PR~ β0 + β1PC3	0.41	0.02		0.00	13.00	3.00	45.60	1.20	0.21

Table 7a. Total inertia (variance) in partial redundancy analysis. Total inertia= total variance in response matrix. Constrained inertia= inertia in response matrix explained by explanatory matrix; unconstrained inertia= unexplained inertia in response variables.

Scale of analysis	Total Inertia	Constrained Inertia	Proportion Constrained Inertia	Unconstrained Inertia	Proportion Unconstrained Inertia
Watershed	1.57	1.35	0.86	0.22	0.14
Riparian	1.57	1.38	0.88	0.19	0.12
4km	1.57	1.41	0.90	0.16	0.10
3.5km	1.57	1.38	0.88	0.19	0.12
3km	1.57	1.31	0.83	0.26	0.17
2.5km	1.57	1.39	0.88	0.18	0.12
2km	1.57	1.40	0.89	0.17	0.11
1.5km	1.57	1.40	0.89	0.17	0.11
1km	1.57	1.40	0.89	0.17	0.11
500m	1.57	1.46	0.93	0.11	0.07

Table 7b. Components results from partial redundancy analysis. Components correspond to a single exclusive (non-overlapping) partition of total response variance. V1=pure effects from burn history matrix; v2= pure effects from geomorphology matrix; v12= joint burn history & geomorphology effects; confounded variance that cannot exclusively be associated with either v1 or v2. Proportion of total= partition size in terms of proportion of total response variance; Proportion of constrained= partition size in terms of proportion of total response variance explained by respective components. *= significant ($p \leq 0.05$), **= marginally significant ($0.25 \geq p > 0.05$)

Scale of analysis	v1 Inertia	v1 Proportion of Total	v1 Proportion of Constrained	v1 p-value	v2 Inertia	v2 Proportion of Total	v2 Proportion of Constrained	v 2 p-value	v12 Inertia	v12 Proportion of Total	v12Proportion of Constrained
Watershed	0.34	0.22	0.25	0.79	0.56	0.36	0.42	0.48	0.45	0.29	0.33
Riparian	0.37	0.23	0.26	0.63	0.68	0.43	0.49	0.30	0.34	0.22	0.25
4km	0.51	0.33	0.36	0.52	0.52	0.33	0.37	0.33	0.37	0.24	0.27
3.5km	0.52	0.33	0.37	0.47	0.51	0.33	0.37	0.54	0.35	0.22	0.25
3km	0.44	0.28	0.34	0.79	0.55	0.35	0.42	0.66	0.32	0.21	0.25
2.5km	0.51	0.33	0.37	0.51	0.58	0.37	0.42	0.41	0.30	0.19	0.21
2km	0.50	0.32	0.36	0.43	0.59	0.38	0.42	0.35	0.31	0.20	0.22
1.5km	0.45	0.29	0.32	0.55	0.58	0.37	0.42	0.30	0.37	0.23	0.26
1km	0.47	0.30	0.33	0.45	0.58	0.37	0.41	0.33	0.35	0.22	0.25
500m	0.57	0.36	0.39	0.15**	0.61	0.39	0.42	0.16**	0.28	0.18	0.19

Table 7c. Marginal effects results from partial redundancy analysis. Marginal effects are total variance in response matrix that can be attributable to a single explanatory matrix without partialling out the potential confounding effect of other explanatory matrices. V1= burn history matrix; v2= geomorphology matrix. Proportion of total = relative effect size given in terms of total response variance; Proportion of constrained = relative effect size in terms of total explained variance. P-values are based on a Monte Carlo test of significance with 1000 random permutations. *= significant ($p \leq 0.05$), **= marginally significant ($0.25 \geq p > 0.05$).

Scale of analysis	v1 Total marginal effect	v1 Proportion of Total	v1 Proportion of Constrained	v1 p-value	v2 Total marginal effect	v2 Proportion of Total	v2 Proportion of Constrained	v2 p-value
Watershed	0.79	0.50	0.58	0.23**	1.01	0.64	0.75	0.01*
Riparian	0.70	0.45	0.51	0.32	1.01	0.65	0.74	0.01*
4km	0.88	0.56	0.63	0.06**	0.89	0.57	0.64	0.05*
3.5km	0.87	0.55	0.63	0.07**	0.86	0.55	0.63	0.09**
3km	0.76	0.48	0.58	0.30	0.87	0.55	0.66	0.07**
2.5km	0.81	0.51	0.58	0.13**	0.88	0.56	0.63	0.06**
2km	0.81	0.52	0.58	0.16**	0.90	0.57	0.64	0.13**
1.5km	0.82	0.52	0.58	0.12**	0.95	0.61	0.68	0.02*
1km	0.82	0.52	0.59	0.11**	0.94	0.60	0.67	0.03*
500m	0.85	0.54	0.58	0.11**	0.89	0.57	0.61	0.05*

References

Acuna, V., A. Giorgi, I. Munoz, U. Uehlinger, and S. Sabater. 2004. Flow extremes and benthic organic matter shape the metabolism of a headwater Mediterranean stream. Freshwater Biology **49**:960-971.

Agee, J. K. 1993. Fire ecology of Pacific Northwest forests. Island Press, Washington, D.C.

Allen, A. P., J. F. Gillooly, and J. H. Brown. 2005. Linking the global carbon cycle to individual metabolism. Functional Ecology **19**:202-213.

Anderson, D. R., and K. P. Burnham. 2002. Avoiding pitfalls when using information-theoretic methods. Journal of Wildlife Management **66**:912-918.

Arkle, R. 2014. *in* E. Davis, editor.

Arkle, R. S., and D. S. Pilliod. 2010. Prescribed fires as ecological surrogates for wildfires: A stream and riparian perspective. Forest Ecology and Management **259**:893-903.

Arkle, R. S., D. S. Pilliod, and K. Strickler. 2010. Fire, flow and dynamic equilibrium in stream macroinvertebrate communities. Freshwater Biology **55**:299-314.

Baxter, C. V. 2014. *in* E. A. Davis, editor.

Bayley, S. E., D. W. Schindler, K. G. Beaty, B. R. Parker, and M. P. Stainton. 1992. EFFECTS OF MULTIPLE FIRES ON NUTRIENT YIELDS FROM STREAMS DRAINING BOREAL FOREST AND FEN WATERSHEDS - NITROGEN AND PHOSPHORUS. Canadian Journal of Fisheries and Aquatic Sciences **49**:584-596.

Benda, L., D. Miller, K. Andras, P. Bigelow, G. Reeves, and D. Michael. 2007. NetMap: A new tool in support of watershed science and resource management. Forest Science **53**:206-219.

Benda, L., N. L. Poff, D. Miller, T. Dunne, G. Reeves, G. Pess, and M. Pollock. 2004. The network dynamics hypothesis: How channel networks structure riverine habitats. Bioscience **54**:413-427.

Bernot, M. J., D. J. Sobota, R. O. Hall, Jr., P. J. Mulholland, W. K. Dodds, J. R. Webster, J. L. Tank, L. R. Ashkenas, L. W. Cooper, C. N. Dahm, S. V. Gregory, N. B. Grimm, S. K. Hamilton, S. L. Johnson, W. H. McDowell, J. L. Meyer, B. Peterson, G. C. Poole, H. M. Valett, C. Arango, J. J. Beaulieu, A. J. Burgin, C. Crenshaw, A. M. Helton, L. Johnson, J. Merriam, B. R. Niederlehner, J. M. O'Brien, J. D. Potter, R. W. Sheibley, S. M. Thomas, and K. Wilson. 2010. Inter-regional comparison of land-use effects on stream metabolism. Freshwater Biology **55**:1874-1890.

Betts, E. F., and J. B. Jones, Jr. 2009. Impact of Wildfire on Stream Nutrient Chemistry and Ecosystem Metabolism in Boreal Forest Catchments of Interior Alaska. Arctic Antarctic and Alpine Research **41**:407-417.

Bott, T. L., J. D. Newbold, and D. B. Arscott. 2006. Ecosystem metabolism in piedmont streams: Reach geomorphology modulates the influence of riparian vegetation. Ecosystems **9**:398-421.

Bunn, S. E., P. M. Davies, and T. D. Mosisch. 1999. Ecosystem measures of river health and their response to riparian and catchment degradation. Freshwater Biology **41**:333-345.

Bunn, S. E., I. R. Tibbetts, N. J. Hall, and W. C. Dennison. 1998a. Riparian influences on ecosystem function in the Brisbane River. School of Marine Science, University of Queensland, Brisbane, Queensland, Australia.

Bunn, S. E., I. R. Tibbetts, N. J. Hall, and W. C. Dennison. 1998b. Riparian influences on ecosystem function in the Brisbane River. Moreton Bay and catchment:131-142.

Burnham, K. P., and D. R. Anderson. 1998. Model selection and inference: A practical information-theoretic approach. Springer-Verlag, Heidelberg, Germany.

Burnham, K. P., D. R. Anderson, K. P. Burnham, and D. R. Anderson. 1998. Model selection and inference: A practical information-theoretic approach. Model selection and inference: A practical information-theoretic approach:xx+353p-xx+353p.

Cole, E., and M. Newton. 2013. Influence of streamside buffers on stream temperature response following clear-cut harvesting in western Oregon. Canadian Journal of Forest Research-Revue Canadienne De Recherche Forestiere **43**:993-1005.

Compton, J. E., M. R. Church, S. T. Larned, and W. E. Hogsett. 2003. Nitrogen export from forested watersheds in the Oregon Coast Range: The role of N(2)-fixing red alder. Ecosystems **6**:773-785.

Cooper, S. D., H. M. Page, S. W. Wiseman, K. Klose, D. Bennett, T. Even, S. Sadro, C. E. Nelson, and T. L. Dudley. 2014. Physicochemical and biological responses of streams to wildfire severity in riparian zones. Freshwater Biology:n/a-n/a.

Davis, J. C., and G. W. Minshall. 1999. Nitrogen and phosphorus uptake in two Idaho (USA) headwater wilderness streams. Oecologia **119**:247-255.

Dunham, J. B., A. E. Rosenberger, C. H. Luce, and B. E. Rieman. 2007. Influences of wildfire and channel reorganization on spatial and temporal variation in stream temperature and the distribution of fish and amphibians. Ecosystems **10**:335-346.

Dwire, K. A., and J. B. Kauffman. 2003. Fire and riparian ecosystems in landscapes of the western USA. Forest Ecology and Management **178**:61-74.

Environmental Systems Resource Institute. 2011. ArcMap 10.1. ESRI, Redlands, California, USA.

Fausch, K. D., C. E. Torgersen, C. V. Baxter, and H. W. Li. 2002. Landscapes to riverscapes: Bridging the gap between research and conservation of stream fishes. Bioscience **52**:483-498.

Fellows, C. S., J. E. Clapcott, J. W. Udy, S. E. Bunn, B. D. Harch, M. J. Smith, and P. M. Davies. 2006. Benthic metabolism as an indicator of stream ecosystem health. Hydrobiologia **572**:71-87.

Finlay, J. C. 2011. Stream size and human influences on ecosystem production in river networks. Ecosphere **2**.

Finlay, J. C., J. M. Hood, M. P. Limm, M. E. Power, J. D. Schade, and J. R. Welter. 2011. Light-mediated thresholds in stream-water nutrient composition in a river network. Ecology **92**:140-150.

Finney, M. A., J. D. Cohen, I. C. Grenfell, and K. M. Yedinak. 2010. An examination of fire spread thresholds in discontinuous fuel beds. International Journal of Wildland Fire **19**:163-170.

Frissell, C. A., W. J. Liss, C. E. Warren, and M. D. Hurley. 1986. A HIERARCHICAL FRAMEWORK FOR STREAM HABITAT CLASSIFICATION - VIEWING STREAMS IN A WATERSHED CONTEXT. Environmental Management **10**:199-214.

Gresswell, R. E. 1999. Fire and aquatic ecosystems in forested biomes of North America. Transactions of the American Fisheries Society **128**:193-221.

Griffiths, N. A., J. L. Tank, T. V. Royer, S. S. Roley, E. J. Rosi-Marshall, M. R. Whiles, J. J. Beaulieu, and L. T. Johnson. 2013. Agricultural land use alters the seasonality and magnitude of stream metabolism. Limnology and Oceanography **58**:1513-1529.

Harris, H. E. 2013. Disturbance cascade: how fire and debris flows affect headwater linkages to downstream and riparian ecosystems. Idaho State University, Pocatello, Idaho, USA.

Hauer, F. R., and C. N. Spencer. 1998. Phosphorus and nitrogen dynamics in streams associated with wildfire: A study of immediate and longterm effects. International Journal of Wildland Fire **8**:183-198.

Heyerdahl, E. K., D. McKenzie, L. D. Daniels, A. E. Hessl, J. S. Littell, and N. J. Mantua. 2008. Climate drivers of regionally synchronous fires in the inland Northwest (1651-1900). International Journal of Wildland Fire **17**:40-49.

Holtgrieve, G. W., and D. E. Schindler. 2011. Marine-derived nutrients, bioturbation, and ecosystem metabolism: reconsidering the role of salmon in streams. Ecology **92**:373-385.

Holtgrieve, G. W., D. E. Schindler, T. A. Branch, and Z. T. A'Mar. 2010. Simultaneous quantification of aquatic ecosystem metabolism and reaeration using a Bayesian statistical model of oxygen dynamics. Limnology and Oceanography **55**:1047-1063.

Hynes, H. B. N. 1974. THE STREAM AND ITS VALLEY. Pages 1-15 *in* International Association of Theoretical and Applied Limnology, Proceedings, Winnipeg, Manitoba, Canada.

Jackson, B. K., and S. M. P. Sullivan. 2009. Influence of wildfire severity on riparian plant community heterogeneity in an Idaho, USA wilderness. Forest Ecology and Management **259**:24-32.

Jackson, B. K., S. M. P. Sullivan, and R. L. Malison. 2012. Wildfire severity mediates fluxes of plant material and terrestrial invertebrates to mountain streams. Forest Ecology and Management **278**:27-34.

Jankowski, K., D. E. Schindler, and P. J. Lisi. 2014. Temperature sensitivity of community respiration rates in streams is associated with watershed geomorphic features. Ecology **95**:2707-2714.

Kiffney, P. M., J. S. Richardson, and J. P. Bull. 2003. Responses of periphyton and insects to experimental manipulation of riparian buffer width along forest streams. Journal of Applied Ecology **40**:1060-1076.

Kiffney, P. M., J. S. Richardson, and J. P. Bull. 2004. Establishing light as a causal mechanism structuring stream communities in response to experimental manipulation of riparian buffer width. Journal of the North American Benthological Society **23**:542-555.

Malison, R. L., and C. V. Baxter. 2010a. Effects of wildfire of varying severity on benthic stream insect assemblages and emergence. Journal of the North American Benthological Society **29**:1324-1338.

Malison, R. L., and C. V. Baxter. 2010b. The fire pulse: wildfire stimulates flux of aquatic prey to terrestrial habitats driving increases in riparian consumers. Canadian Journal of Fisheries and Aquatic Sciences **67**:570-579.

McTammany, M. E., E. F. Benfield, and J. R. Webster. 2007. Recovery of stream ecosystem metabolism from historical agriculture. Journal of the North American Benthological Society **26**:532-545.

Minshall, G. W. 2003. Responses of stream benthic macroinvertebrates to fire. Forest Ecology and Management **178**:155-161.

Minshall, G. W., J. T. Brock, and J. D. Varley. 1989. WILDFIRES AND YELLOWSTONE STREAM ECOSYSTEMS. Bioscience **39**:707-715.

Mosisch, T. D., S. E. Bunn, and P. M. Davies. 2001. The relative importance of shading and nutrients on algal production in subtropical streams. Freshwater Biology **46**:1269-1278.

Mulholland, P. J., C. S. Fellows, J. L. Tank, N. B. Grimm, J. R. Webster, S. K. Hamilton, E. Marti, L. Ashkenas, W. B. Bowden, W. K. Dodds, W. H. McDowell, M. J. Paul, and B. J. Peterson. 2001. Inter-biome comparison of factors controlling stream metabolism. Freshwater Biology **46**:1503-1517.

Newton, M., and L. Cole. 2013. Stream Temperature and Streamside Cover 14-17 Years after Clearcutting along Small Forested Streams, Western Oregon. Western Journal of Applied Forestry **28**:107-115.

Odum, H. T. 1956. PRIMARY PRODUCTION IN FLOWING WATERS. Limnology and Oceanography **1**:102-117.

Parks, S. A., G. K. Dillon, and C. Miller. 2014a. A New Metric for Quantifying Burn Severity: The Relativized Burn Ratio. Remote Sensing **6**:1827-1844.

Parks, S. A., C. Miller, C. R. Nelson, and Z. A. Holden. 2014b. Previous Fires Moderate Burn Severity of Subsequent Wildland Fires in Two Large Western US Wilderness Areas. Ecosystems **17**:29-42.

Peterson, E. E., F. Sheldon, R. Darnell, S. E. Bunn, and B. D. Harch. 2011. A comparison of spatially explicit landscape representation methods and their relationship to stream condition. Freshwater Biology **56**:590-610.

Pettit, N. E., and R. J. Naiman. 2007. Fire in the riparian zone: Characteristics and ecological consequences. Ecosystems **10**:673-687.

Pierce, J. L., G. A. Meyer, and A. J. T. Jull. 2004. Fire-induced erosion and millennialscale climate change in northern ponderosa pine forests. Nature **432**:87-90.

R Development Core Team. 2012. R: A language and environment for statistical computing. R Foundation for Statistical Computing, Vienna, Austria.

Ramirez, A., C. M. Pringle, and L. Molina. 2003. Effects of stream phosphorus levels on microbial respiration. Freshwater Biology **48**:88-97.

Rieman, B., J. B. Dunham, and J. Clayton. 2006. Emerging concepts for management of river ecosystems and challenges to applied integration of physical and biological sciences in the Pacific Northwest, USA. International Journal of River Basin Management **4**:85-97.

Robinson, C. T., and U. Uehlinger. 2008. Experimental floods cause ecosystem regime shift in a regulated river. Ecological Applications **18**:511-526.

Robinson, C. T., U. Uehlinger, and G. W. Minshall. 2005. Functional characteristics of wilderness streams twenty years following wildfire. Western North American Naturalist **65**:1-10.

Robinson, C. T., U. Uehlinger, and M. T. Monaghan. 2004. Stream ecosystem response to multiple experimental floods from a reservoir. River Research and Applications **20**:359-377.

Romme, W. H., M. S. Boyce, R. Gresswell, E. H. Merrill, G. W. Minshall, C. Whitlock, and M. G. Turner. 2011. Twenty Years After the 1988 Yellowstone Fires: Lessons About Disturbance and Ecosystems. Ecosystems **14**:1196-1215.

Rosenberger, A. E., J. B. Dunham, J. M. Buffington, and M. S. Wipfli. 2011. Persistent Effects of Wildfire and Debris Flows on the Invertebrate Prey Base of Rainbow Trout in Idaho Streams. Northwest Science **85**:55-63.

Rutherford, J. C., N. A. Marsh, P. M. Davies, and S. E. Bunn. 2004. Effects of patchy shade on stream water temperature: how quickly do small streams heat and cool? Marine and Freshwater Research **55**:737-748.

Sheldon, F., E. E. Peterson, E. L. Boone, S. Sippel, S. E. Bunn, and B. D. Harch. 2012. Identifying the spatial scale of land use that most strongly influences overall river ecosystem health score. Ecological Applications **22**:2188-2203.

Tuckett, Q. 2007. The Effects of Wildfire and Debris Flows on Small Headwater Stream Ecosystems in Central Idaho. Boise State University, Boise, Idaho.

Uehlinger, U., B. Kawecka, and C. T. Robinson. 2003. Effects of experimental floods on periphyton and stream metabolism below a high dam in the Swiss Alps (River Spol). Aquatic Sciences **65**:199-209.

UNESCO. 1994. Protocols for the joint global ocean flux study (JGOFS) core measurements. Page 181 *in* I. O. Commission, editor. UNESCO, Paris, France.

Valderrama, J. C. 1981. THE SIMULTANEOUS ANALYSIS OF TOTAL NITROGEN AND TOTAL PHOSPHORUS IN NATURAL-WATERS. Marine Chemistry **10**:109-122.

Vannote, R. L., G. W. Minshall, K. W. Cummins, J. R. Sedell, and C. E. Cushing. 1980. RIVER CONTINUUM CONCEPT. Canadian Journal of Fisheries and Aquatic Sciences **37**:130-137.

Verkaik, I., M. Rieradevall, S. D. Cooper, J. M. Melack, T. L. Dudley, and N. Prat. 2013. Fire as a disturbance in mediterranean climate streams. Hydrobiologia **719**:353-382.

Yates, A. G., R. B. Brua, J. M. Culp, and P. A. Chambers. 2013. Multi-scaled drivers of rural prairie stream metabolism along human activity gradients. Freshwater Biology **58**:675-689.

Young, R. G., and A. D. Huryn. 1996. Interannual variation in discharge controls ecosystem metabolism along a grassland river continuum. Canadian Journal of Fisheries and Aquatic Sciences **53**:2199-2211.

Young, R. G., and A. D. Huryn. 1999. Effects of land use on stream metabolism and organic matter turnover. Ecological Applications **9**:1359-1376.

Acknowledgements

This project would not have been possible without the help and support of many people. Funding was provided by the National Science Foundation Graduate Research Fellowship Program, the Northwest Scientific Association, the H. Mason Keeler Memorial Fund, and the Harriett Bullitt Endowment. Each of my committee members brought something different to the table, and I feel lucky to have worked with such renowned ecologists. In particular I would like to thank my advisor Daniel Schindler for supporting this unorthodox project and allowing me so much latitude in my graduate work. Thanks to Si Simenstad for providing your expert perspective on ecosystem ecology and your quick turnaround on thesis drafts. Thanks to Christian Torgersen for your expertise in ecological scaling, your kind and patient nature, and your attention to detail. Thanks to Colden Baxter for being willing to collaborate with me, enabling my fieldwork at Taylor Ranch, granting me access to your lab staff and equipment, and always being willing to discuss ideas over the phone. Jenna Keeton was an incredibly helpful, enthusiastic, and cheerful field assistant without whose positive attitude I never would have survived my 2013 field season. The following people and institutions provided invaluable help with logistics and equipment: all staff at Taylor Ranch Wilderness Research Station the Idaho State University Center for Ecological Research, UW Marine Chemistry Laboratory, and University of Idaho's College of Natural Resources. The intrepid staff and pilots at Arnold Aviation made it possible for me to safely travel into one of the most remote and inaccessible places in the lower 48 with hundreds of pounds of gear. Kate Rowe and Patricia Haggerty answered countless questions about GIS, and Lee Benda and Dan Miller granted me access to TerrainWorks' NetMap GIS tools for free. Sean Parks and Alina Cansler provided fire ecology advice and access to crucial fire mapping data. Loveday Conquest, Kiva Oken, and Julian Olden assisted with my many statistical

quandaries. Gordon Holtgrieve patiently endured my constant pestering about BaMM and stream metabolism. Thanks to Robert Arkle and Breanne “Breezy” Jackson for teaching me about your work with fire and streams, being a sounding board for my ideas and providing great visuals for my defense. Without the SAFS admin office to help me with logistics of travel, budgets, and scholarships, I would have been up a creek without a paddle—thank you all. Amy Fox provided invaluable moral support in times of crisis. KathiJo Jankowski provided helpful comments on this manuscript, helped me learn BaMM, and was an all-around awesome and supportive scientific role model. Liza Mitchell, Marissa Jones, Aubrey Gallegos, Tala Woodward, and the members of Book Club were my sanity release valve and moral support. My family is owed a huge debt of gratitude for all the unconditional love and encouragement even when it seemed like I might be totally losing it. Finally, thanks to all Schindler lab members past and present, and the entire SAFS graduate student community for years of support, inspiration, and laughter.

Appendix 1: Supplemental Figures

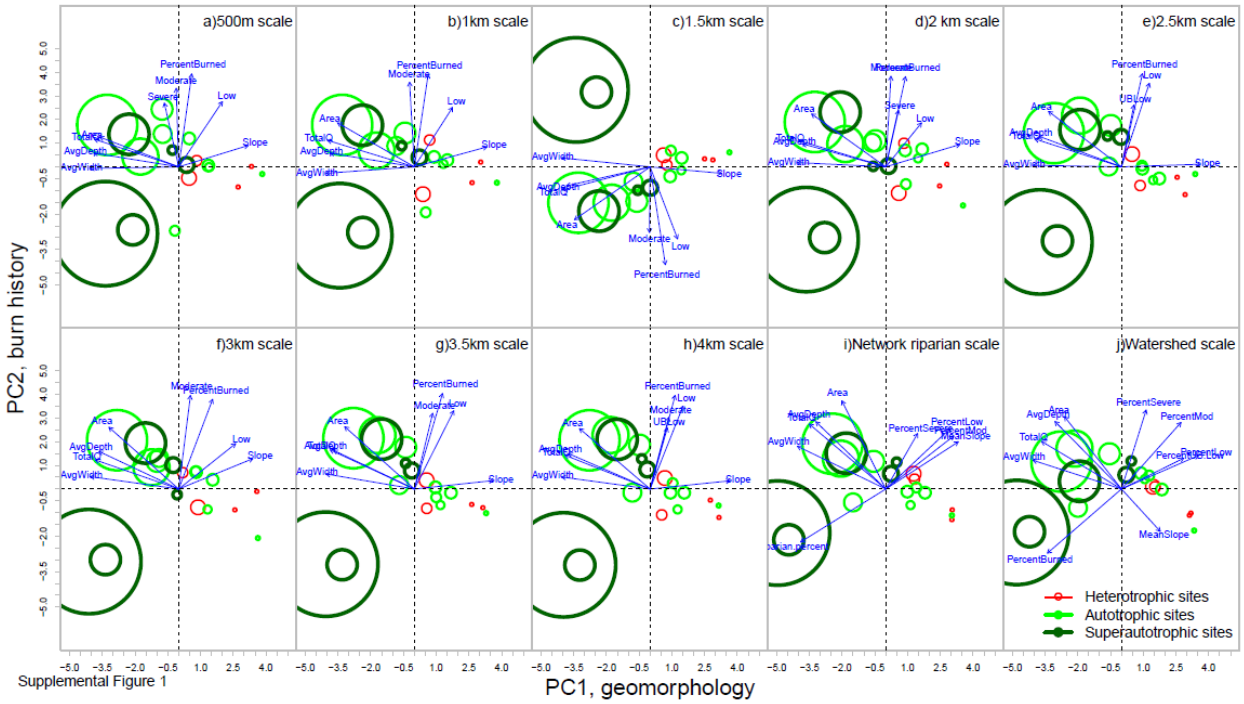

Supplemental Figure 4 a-j. Principal component analyses for environmental data (stream geomorphology and burn history) for each of 10 spatial resolutions: a) 500-m riparian buffer (PC1 43.57%, PC2 22.91%); b) 1000-m riparian buffer (PC1 43.74%, PC2 20.32%); c) 1500-m riparian buffer (PC1 42.79%, PC2 20.33%); d) 2000-m riparian buffer (PC1 43.86%, PC2 22.5%); e) 2500-m riparian buffer (PC1 43.91%, PC2 22.91%); f) 3000-m riparian buffer (PC1 47.44%, PC2 23.41%); g) 3500-m riparian buffer (PC1 44.35%, PC2 25.46%); h) 4000-m riparian buffer (PC1 43.85%, PC2 26.4%); i) network-scale riparian buffer (PC1 58.25%, PC2 16.42%); j) watershed scale (PC1 60.85%, PC2 15.9%). 'PC'= principal component. All vectors shown are significant. 'TotalQ'=stream discharge; 'AvgWidth'= mean stream width; 'AvgDepth'=mean stream depth; 'Slope'=mean slope over study area; 'PercentLow'=percent area burned with low severity; 'PercentMod'=percent area burned with moderate severity; 'PercentSevere'=percent area burned with high severity; 'PercentUB'=percent area burned with very low severity. Open circles, which represent stream sites, are scaled by the mean width of the stream.

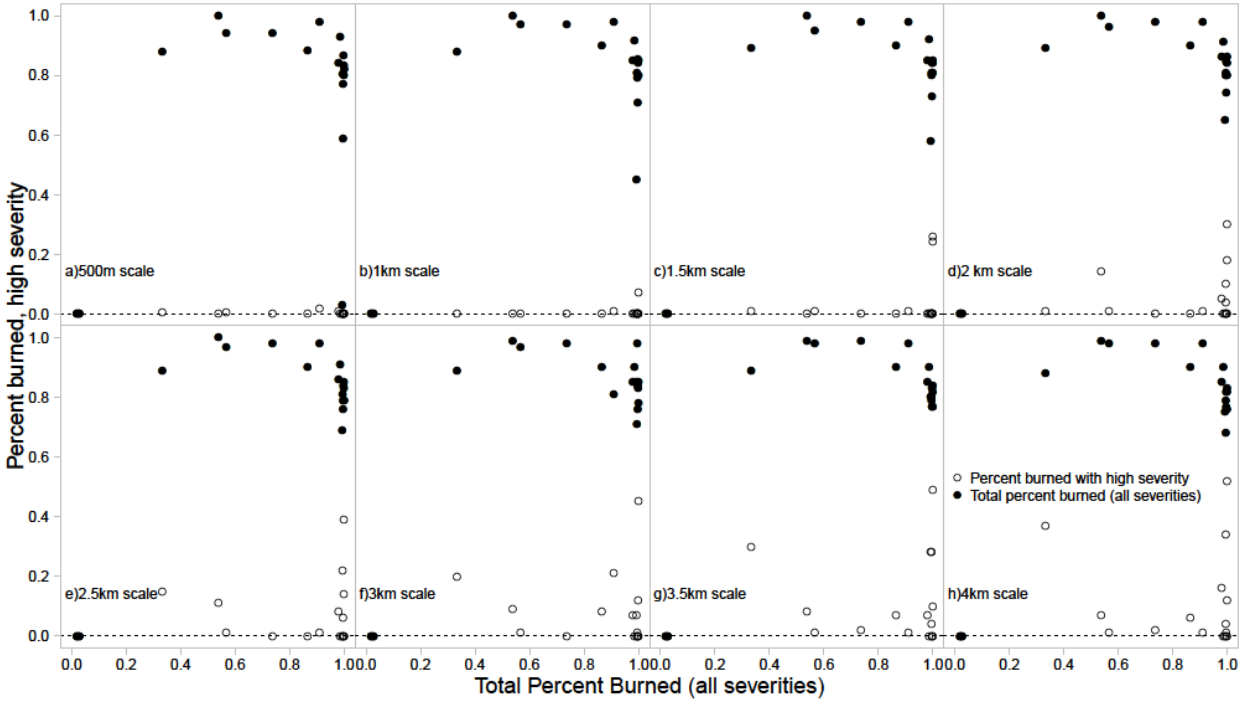

Supplemental Figure 5 a-h. Percent watershed burned plotted against total percent of riparian buffer burned, and percent of buffer burned at high severity, over 8 spatial scales of riparian buffer: a) 500-m; b) 1000-m; c) 1500-m; d) 2000-m; e) 2500-m; f) 3000-m; g) 3500-m h) 4000-m.

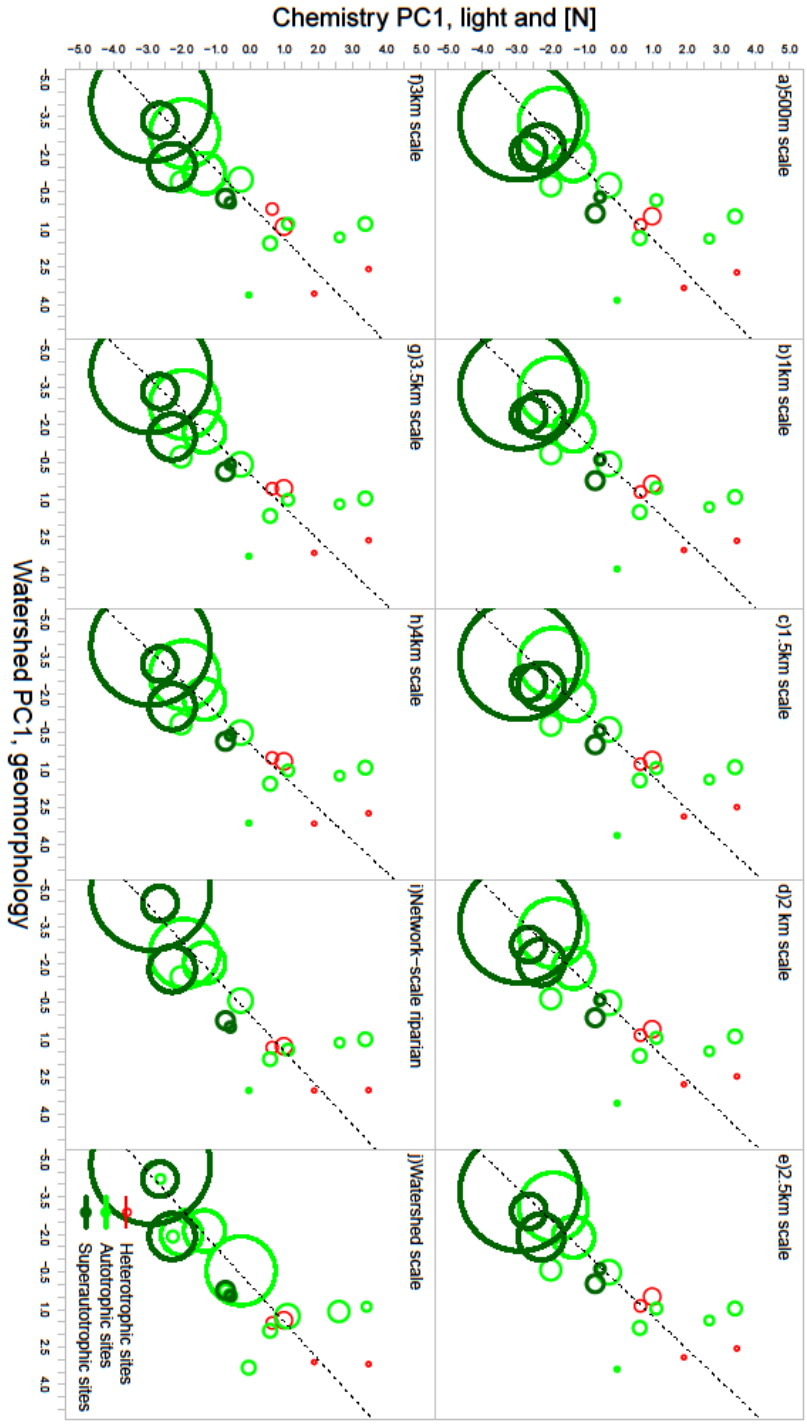

Supplemental Figure 6a-j. Principal component regressions of response principal component 1 (light and nitrogen concentration) against explanatory principal component 1 (stream geomorphology) for each of ten spatial scales of analysis: a) watershed; b) network-scale riparian buffer; c) 4000-m riparian buffer; d) 3500-m riparian buffer; e) 3000-m riparian buffer; f) 2500-m riparian buffer; g) 2000-m riparian buffer; h) 1500-m riparian buffer; i) 1000-m riparian buffer; j) 500-m riparian buffer. 'PC'= principal component. Open circles, which represent streams, are scaled by the mean width of the stream.